

# Prediction-Powered Adaptive Shrinkage Estimation

Sida Li  
listar2000@uchicago.edu

Nikolaos Ignatiadis  
ignat@uchicago.edu

Draft Manuscript, February 2025

## Abstract

Prediction-Powered Inference (PPI) is a powerful framework for enhancing statistical estimates by combining limited gold-standard data with machine learning (ML) predictions. While prior work has demonstrated PPI's benefits for individual statistical problems, modern applications require answering numerous parallel statistical questions. We introduce Prediction-Powered Adaptive Shrinkage (PAS), a method that bridges PPI with empirical Bayes shrinkage to improve estimation of multiple means. PAS debiases noisy ML predictions *within* each problem and then borrows strength *across* problems by using those same predictions as a reference point for shrinkage. The amount of shrinkage is determined by minimizing an unbiased estimate of risk, and we prove that this tuning strategy is asymptotically optimal. Experiments on both synthetic and real-world datasets show that PAS adapts to the reliability of the ML predictions and outperforms traditional and modern baselines in large-scale applications.

## 1 Introduction

A major obstacle in answering modern scientific questions is the scarcity of gold-standard data [Miao et al., 2024b]. While advancements in data collection, such as large-scale astronomical surveys [York et al., 2000] and web crawling [Penedo et al., 2024], have led to an abundance of covariates (or features), scientific conclusions often rely on outcomes (or labels), which are often expensive and labor-intensive to obtain. The rapid development of machine learning (ML) algorithms has offered a path forward, with ML predictions increasingly used to supplement gold-standard outcomes and increase the statistical efficiency of subsequent analyses [Liang et al., 2007, Wang et al., 2020].

Prediction-Powered Inference (PPI) [Angelopoulos et al., 2023] addresses the scarcity issue by providing a framework for valid statistical analysis using predictions from black-box ML models. By combining ML-predicted and gold-standard outcomes, PPI and its variants [Angelopoulos et al., 2024, Zrnic and Candès, 2024, Zrnic, 2025] use the abundance of predictions to reduce variance while relying on the accuracy of labeled<sup>1</sup> data to control bias.

In this work, we adapt PPI to the estimation of multiple outcome means in compound estimation settings. Many applications of PPI naturally involve parallel statistical problems that can be solved simultaneously. For instance, several PPI methods [Angelopoulos et al., 2024, Fisch et al., 2024] have shown improvements in estimating the fraction of spiral galaxies using predictions on images from the Galaxy Zoo 2 dataset [Willett et al., 2013]. While these methods focus on estimating a single overall fraction, a richer analysis emerges from partitioning galaxies based on metadata (such as celestial coordinates or pre-defined bins) and estimating the fraction of galaxies within each partition. This compound estimation approach enables more granular scientific inquiries that account for heterogeneity across galaxy clusters and spatial locations [Nair and Abraham, 2010].

We demonstrate, both theoretically and empirically, the benefits of solving multiple mean estimation problems simultaneously. Our approach builds on the empirical Bayes principle of sharing information *across* problems [Robbins, 1956, Efron, 2010] as exemplified by James-Stein shrinkage [James and Stein, 1961, Xie et al., 2012]. The connection between modern and classical statistical ideas allows us to

---

<sup>1</sup>Throughout the paper, we will use the terms “labeled” and “gold-standard” interchangeably.

perform *within* problem PPI estimation in the first place, followed by a shrinkage process reusing the ML predictions in an adaptive manner, which becomes possible through borrowing information *across* problems. Our contributions are as follows:

1. We propose Prediction-Powered Addaptive Shrinkage (**PAS**) for compound mean estimation. **PAS** inherits the flexibility of PPI in working with any black-box predictive model and makes minimal distributional assumptions about the data. Its two-stage estimation process makes efficient use of the ML predictions as both a variance-reduction device and a shrinkage target.
2. We develop a Correlation-Aware Unbiased Risk Estimate (CURE) for tuning the **PAS** estimator, establish asymptotic optimality of this tuning strategy, and derive an interpretation in terms of a Bayes oracle risk upper bound.
3. We conduct extensive experiments on both synthetic and real-world datasets. Our experiments demonstrate **PAS**'s applicability to large-scale problems with deep learning models, showing improved estimation accuracy compared to other estimators (e.g., classical, PPI++).

## 2 Preliminaries and Notation

### 2.1 Prediction-Powered Inference (PPI)

The PPI framework considers a setting where we have access to a small number of labeled data points  $(X_i, Y_i)_{i=1}^n \in (\mathcal{X} \times \mathcal{Y})^n$  and a large number of unlabeled covariates  $(\tilde{X}_i)_{i=1}^N \in (\mathcal{X})^N$ , where  $\mathcal{X}$  and  $\mathcal{Y}$  represent the covariate and outcome space, respectively. The data points are drawn iid from a joint distribution  $\mathbb{P}_{XY}$ .<sup>2</sup> We are also given a black-box predictive model  $f : \mathcal{X} \rightarrow \mathcal{Y}$  that is independent of the datasets (e.g., pre-trained on similar but unseen data). For mean estimation with  $\mathcal{Y} \subset \mathbb{R}$ , the goal is to leverage the predicted outcomes  $f(X_i)$  to improve the estimation of  $\theta := \mathbb{E}[Y_i]$ . Some simple estimators take the form of the following aggregated (summary) statistics

$$\begin{aligned} \bar{Y} &:= \frac{1}{n} \sum_{i=1}^n Y_i, & \tilde{Y} &:= \frac{1}{N} \sum_{i=1}^N \tilde{Y}_i, \\ \bar{Z}^f &:= \frac{1}{n} \sum_{i=1}^n f(X_i), & \tilde{Z}^f &:= \frac{1}{N} \sum_{i=1}^N f(\tilde{X}_i). \end{aligned} \tag{1}$$

Above,  $\bar{Y}$  is the classical estimator,<sup>3</sup>  $\bar{Z}^f, \tilde{Z}^f$  are the prediction means on the labeled and unlabeled data, and  $\tilde{Y}$  (greyed out) is unobserved. The vanilla PPI estimator is defined as,

$$\hat{\theta}^{\text{PPI}} := \underbrace{\bar{Y}}_{\text{Baseline}} + \underbrace{(\tilde{Z}^f - \bar{Z}^f)}_{\text{Variance Reduction}} = \underbrace{\tilde{Z}^f}_{\text{Baseline}} + \underbrace{(\bar{Y} - \tilde{Z}^f)}_{\text{Debiasing}}. \tag{2}$$

Both definitions represent  $\hat{\theta}^{\text{PPI}}$  in the form of a **baseline estimator** plus a **correction term**. In the first representation, the baseline estimator is the unbiased classical estimator  $\bar{Y}$ , while the correction term has expectation 0 and attempts to reduce the variance of  $\bar{Y}$ . In the second representation, the baseline estimator is the prediction mean on unlabeled data  $\tilde{Z}^f$  (which in general may be biased for  $\theta$ ), while the correction term removes the bias of  $\tilde{Z}^f$  by estimating the bias of the ML model  $f$  on the labeled dataset. Writing  $\hat{\theta}^{\text{PPI}} = \frac{1}{N} \sum_{i=1}^N f(\tilde{X}_i) + \frac{1}{n} \sum_{i=1}^n (Y_i - f(X_i))$ , we find

$$\begin{aligned} \mathbb{E}[\hat{\theta}^{\text{PPI}}] &= \mathbb{E}[Y_i] = \theta, \\ \text{Var}[\hat{\theta}^{\text{PPI}}] &= \frac{1}{N} \text{Var}[f(\tilde{X}_i)] + \frac{1}{n} \text{Var}[Y_i - f(X_i)], \end{aligned} \tag{3}$$

that is,  $\hat{\theta}^{\text{PPI}}$  is unbiased for  $\theta$  and its variance becomes smaller when the model predicts the true outcomes well. The mean squared error (MSE) of  $\hat{\theta}^{\text{PPI}}$  is equal to  $\text{Var}[\hat{\theta}^{\text{PPI}}]$ . Although we motivated  $\hat{\theta}^{\text{PPI}}$  in (2) as implementing a correction step on two possible baseline estimators ( $\bar{Y}$  and  $\tilde{Z}^f$ ),  $\hat{\theta}^{\text{PPI}}$  may have MSE for estimating  $\theta$  that is arbitrarily worse than either of these baselines.

<sup>2</sup>To be concrete:  $(X_i, Y_i) \stackrel{\text{iid}}{\sim} \mathbb{P}_{XY}$  and  $(\tilde{X}_i, \tilde{Y}_i) \stackrel{\text{iid}}{\sim} \mathbb{P}_{XY}$ , but  $\tilde{Y}_i$  is unobserved.

<sup>3</sup>From now on, we will use the term ‘‘classical estimator’’ to refer to the sample average of the labeled outcomes.

**Comparison to classical estimator  $\bar{Y}$ .** The classical estimator  $\bar{Y}$  which only uses labeled data is unbiased for  $\theta$  and has variance (and MSE) equal to  $n^{-1}\text{Var}[Y_i]$ , while the MSE of  $\hat{\theta}^{\text{PPI}}$  in (3) may be arbitrarily large when the predictive model is inaccurate.

**Power-Tuned PPI (PPI++).** To overcome the above limitation, Angelopoulos et al. [2024] introduce a power-tuning parameter  $\lambda$  and define

$$\hat{\theta}_\lambda^{\text{PPI}} := \bar{Y} + \lambda \left( \tilde{Z}^f - \bar{Z}^f \right), \quad (4)$$

which recovers the classical estimator when  $\lambda = 0$  and the vanilla PPI estimator when  $\lambda = 1$ . For all values of  $\lambda$ ,  $\hat{\theta}_\lambda^{\text{PPI}}$  is unbiased, so if we select the  $\lambda$  that minimizes  $\text{Var}[\hat{\theta}_\lambda^{\text{PPI}}]$ , we can improve our estimator over both the classical estimator and vanilla PPI. Such an estimator is defined as the Power-Tuned PPI (PT<sup>4</sup>) estimator  $\hat{\theta}^{\text{PT}} := \hat{\theta}_{\lambda^*}^{\text{PPI}}$ , where

$$\lambda^* := \arg \min_{\lambda \in [0,1]} \text{Var}[\hat{\theta}_\lambda^{\text{PPI}}].$$

Power-tuning will be one of the building blocks of PAS in Section 4.

**Comparison to  $\tilde{Z}^f$ .** Consider the ideal scenario for PPI with  $N = \infty$  (that is, the unlabeled dataset is much larger than the labeled dataset) so that  $\tilde{Z}^f \equiv \mathbb{E}[f(\tilde{X}_i)]$ . Even then, the MSE of  $\hat{\theta}^{\text{PPI}}$  in (3) is always lower bounded<sup>5</sup> by  $\mathbb{E}[\text{Var}[Y_i | X_i]]/n$  and the lower bound is attained for the perfect ML predictor  $f(\cdot) \equiv \mathbb{E}[Y_i | X_i = \cdot]$ . In words, if  $Y_i$  is not perfectly predictable from  $X_i$ , then PPI applied to a labeled dataset of fixed size  $n$  must have nonnegligible MSE. By contrast, for  $N = \infty$ , the prediction mean of unlabeled data  $\tilde{Z}^f$  has zero variance and MSE equal to the squared bias  $(\mathbb{E}[f(X_i)] - \theta_i)^2$ . Thus if the predictor satisfies a calibration-type property that  $\mathbb{E}[f(X_i)] \approx \mathbb{E}[Y_i]$  (which is implied by, but much weaker than the requirement  $f(X_i) \approx Y_i$ ), then the MSE of  $\tilde{Z}^f$  could be nearly 0. By contrast, PPI (and PPI++) can only partially capitalize on such a predictor  $f(\cdot)$ .

While PPI and PPI++ are constrained by their reliance on unbiased estimators, we show that the compound estimation setting (Section 2.2) enables a different approach. By carefully navigating the bias-variance tradeoff through information sharing *across* parallel estimation problems, we can provably match the performance of both  $\bar{Y}$  and  $\tilde{Z}^f$ .

## 2.2 The Compound Mean Estimation Setting

In this section, we introduce the problem setting that PAS is designed to address—estimating the mean of  $m > 1$  parallel problems with a single black-box predictive model  $f$ .<sup>6</sup> For the  $j$ -th problem, where  $j \in [m] := \{1, \dots, m\}$ , we observe a labeled dataset  $(X_{ij}, Y_{ij})_{i=1}^{n_j}$  with  $n_j \in \mathbb{N}$  observations and an unlabeled dataset  $(\tilde{X}_{ij})_{i=1}^{N_j}$  with  $N_j \in \mathbb{N}$  observations. We start with modeling heterogeneity across problems.

**Assumption 2.1** (Prior). There exist problem-specific unobserved latent variables  $\eta_j$  with

$$\eta_j \stackrel{\text{iid}}{\sim} \mathbb{P}_\eta, \quad j \in [m], \quad \text{and} \quad \boldsymbol{\eta} := (\eta_1, \dots, \eta_m)^\top, \quad (5)$$

where  $\mathbb{P}_\eta$  is an unknown probability measure. The latent variable  $\eta_j$  fully specifies the distribution of the  $j$ -th labeled and unlabeled dataset. We use the notation  $\mathbb{E}_{\eta_j}[\cdot]$  (resp.  $\mathbb{E}_\eta[\cdot]$ ) to denote the expectation conditional on  $\eta_j$  (resp.  $\boldsymbol{\eta}$ ), while  $\mathbb{E}_{\mathbb{P}_\eta}[\cdot]$  denotes an expectation also integrating out  $\mathbb{P}_\eta$ .

We do not place any restriction over the unknown prior  $\mathbb{P}_\eta$ . Assumption 2.1 posits exchangeability across problems, which enables information sharing, without restricting heterogeneity [Ignatiadis et al., 2023]. In our setting, we are specifically interested in the means

$$\theta_j := \mathbb{E}_{\eta_j}[Y_{ij}], \quad j \in [m], \quad \text{and} \quad \boldsymbol{\theta} := (\theta_1, \dots, \theta_m)^\top. \quad (6)$$

<sup>4</sup>We will use the term ‘‘PPI++’’ for the larger framework, while ‘‘PT’’ refers to the specific estimator.

<sup>5</sup>The same lower bound also applies to power-tuned PPI  $\hat{\theta}^{\text{PT}}$ .

<sup>6</sup>Our proposal also accommodates using separate predictors  $\{f_j\}_{j=1}^m$  for each problem. To streamline exposition, we focus on the practical scenario where a single (large) model (e.g., an LLM or vision model) can handle multiple tasks simultaneously [Radford et al., 2019, He et al., 2022].

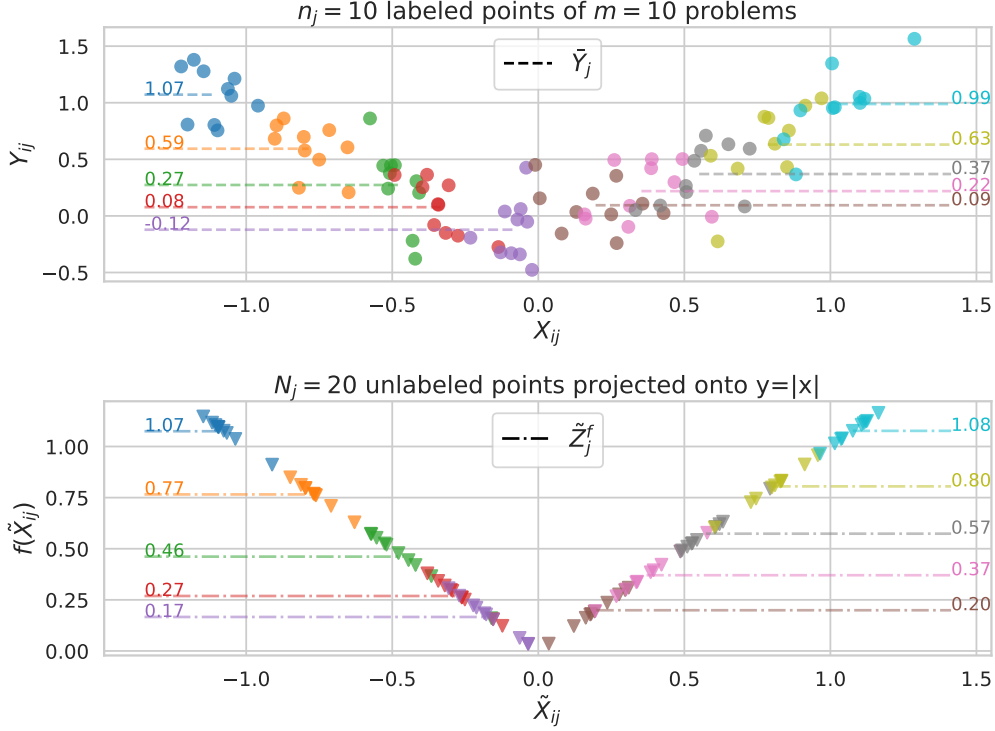


Figure 1: We instantiate the model described in Example 2.3 with  $m = 10$  problems, each has  $n_j = 10$  labeled and  $N_j = 20$  unlabeled data (in different colors). (Top) Labeled data  $(X_{ij}, Y_{ij})_{j=1}^{n_j}$  with the classical estimator  $\bar{Y}_j$  shown for each problem. (Bottom) We apply a flawed predictor  $f(x) = |x|$  to the unlabeled covariates and visualize  $(X_{ij}, f(X_{ij}))_{j=1}^{N_j}$  as well as the prediction mean  $\tilde{Z}_j^f$ .

Our next assumption specifies that we only model the first two moments of the joint distribution between the outcomes and the predictions. The upshots of such modeling are that the exact form of the observation distribution is neither assumed nor required in our arguments, and that our approach will be directly applicable to settings where the covariate space  $\mathcal{X}$  is high-dimensional or structured.

**Assumption 2.2** (Sampling). For each problem  $j \in [m]$ , we assume that the joint distribution of  $(f(X_{ij}), Y_{ij})$  has finite second moments conditional on  $\eta_j$  and that

$$\begin{bmatrix} f(X_{ij}) \\ Y_{ij} \end{bmatrix} \mid \eta_j \stackrel{\text{iid}}{\sim} \mathbb{F}_j \left( \begin{bmatrix} \mu_j \\ \theta_j \end{bmatrix}, \begin{bmatrix} \tau_j^2 & \rho_j \tau_j \sigma_j \\ \rho_j \tau_j \sigma_j & \sigma_j^2 \end{bmatrix} \right), \quad i \in [n_j], \quad (7)$$

where  $\mathbb{F}_j, \mu_j, \theta_j, \rho_j, \sigma_j^2, \tau_j^2$  are functions of  $\eta_j$ . Conditional on  $\eta_j$ , the unlabeled predictions  $f(\tilde{X}_{i'j})$ ,  $i' \in [N_j]$ , are also iid, independent of the labeled dataset and identically distributed with  $f(X_{ij})$ . In the notation of (7),  $\mathbb{F}_j$  represents a unspecified distribution satisfying the moment constraints in (6) and

$$\begin{aligned} \mathbb{E}_{\eta_j}[f(X_{ij})] &= \mu_j, & \text{Var}_{\eta_j}[f(X_{ij})] &= \tau_j^2, \\ \text{Corr}_{\eta_j}[f(X_{ij}), Y_{ij}] &= \rho_j, & \text{Var}_{\eta_j}[Y_{ij}] &= \sigma_j^2. \end{aligned}$$

We further denote  $\gamma_j := \text{Cov}_{\eta_j}[f(X_{ij}), Y_{ij}] = \rho_j \tau_j \sigma_j$ .

Similar to Eq. (1), we define the aggregated statistics  $\bar{Y}_j, \bar{Z}_j^f, \tilde{Z}_j^f$  for each  $j \in [m]$ . Following prior work,<sup>7</sup> we treat  $\tau_j, \sigma_j, \rho_j$  as known in our development. The rationale is that estimation of  $\tau_j, \sigma_j, \rho_j$  is a second-order concern in our setup of mean estimation and treating these as known facilitates exposition. In practice, such as in our numerical experiments with real-world datasets, we use sample-based estimates of  $\tau_j, \sigma_j$ , and  $\rho_j$  (see Appendix D.1).

We next introduce a synthetic model that will serve both as a running example and as part of our numerical study.

<sup>7</sup>For EB, examples include Xie et al. [2012], Soloff et al. [2024]; for PPI, see recent works like Fisch et al. [2024].

**Example 2.3 (Synthetic model).** For each problem  $j$ , let  $\eta_j \sim \mathcal{U}[-1, 1]$ . We think of  $\eta_j$  as both indexing the problems, and generating heterogeneity across problems. The  $j$ -th dataset is generated via (with constants  $c = 0.05, \psi = 0.1$ ),

$$X_{ij} \stackrel{\text{iid}}{\sim} \mathcal{N}(\eta_j, \psi^2), \quad Y_{ij}|X_{ij} \stackrel{\text{iid}}{\sim} \mathcal{N}(2\eta_j X_{ij} - \eta_j^2, c). \quad (8)$$

In Figure 1, we visualize realizations from this model with  $m = 10$  problems,  $n_j = 10$  labeled observations, and  $N_j = 20$  unlabeled observations for each problem. We apply a flawed predictor  $f(x) = |x|$ . The classical estimator  $\bar{Y}_j$  and the prediction mean  $\tilde{Z}_j^f$  deviate from each other. Nevertheless,  $\tilde{Z}_j^f$  contains information that can help us improve upon  $\bar{Y}_j$  as an estimator of  $\theta_j$  by learning from within problem (PPI, PPI++, this work) and across problem (this work) structure. We emphasize that as specified in (7), our approach only requires modeling the first and second moments of the joint distribution of  $(f(X_{ij}), Y_{ij})$ . For instance, in this synthetic model,  $\theta_j = \eta_j^2$  and  $\sigma_j^2 = 4\eta_j^2\psi^2 + c$ , while  $\mu_j, \tau_j^2$  and  $\gamma_j$  also admit closed-form expressions in terms of  $\eta_j$  when the predictor takes the form  $f(x) = |x|$  or  $f(x) = x^2$  (see Appendix D.2).

To conclude this section, we define the compound risk [Robbins, 1951, Jiang and Zhang, 2009] for any estimator  $\hat{\boldsymbol{\theta}} = (\hat{\theta}_1, \dots, \hat{\theta}_m)^\top$  as the expected squared error loss averaged over problems,

$$\mathcal{R}_m(\hat{\boldsymbol{\theta}}, \boldsymbol{\theta}) := \mathbb{E}_\eta \left[ \ell_m(\hat{\boldsymbol{\theta}}, \boldsymbol{\theta}) \right], \quad (9)$$

$$\text{where } \ell_m(\hat{\boldsymbol{\theta}}, \boldsymbol{\theta}) := \frac{1}{m} \sum_{j=1}^m (\hat{\theta}_j - \theta_j)^2. \quad (10)$$

The Bayes risk, which we also refer to simply as mean squared error (MSE), further integrates over randomness in the unknown prior  $\mathbb{P}_\eta$  in (5),

$$\mathcal{B}_m^{\mathbb{P}_\eta}(\hat{\boldsymbol{\theta}}) := \mathbb{E}_{\mathbb{P}_\eta} \left[ \mathcal{R}_m(\hat{\boldsymbol{\theta}}, \boldsymbol{\theta}) \right]. \quad (11)$$

### 3 Statistical Guiding Principles and Connections to Prior Work

In this section, we illustrate both the statistical guiding principles of our approach and some connections to prior work through the following stylized Gaussian model:

$$\begin{aligned} \text{Sampling: } & \hat{\theta}^{\text{cl}} = \theta + (\xi + \varepsilon), \quad \xi \sim \mathcal{N}(0, \sigma_\xi^2), \quad \varepsilon \sim \mathcal{N}(0, \sigma_\varepsilon^2). \\ \text{Prior: } & \theta \sim \mathcal{N}(0, \sigma_\theta^2), \quad \phi \sim \mathcal{N}(0, \sigma_\phi^2), \quad \text{Corr}[\theta, \phi] = \rho. \end{aligned}$$

In our stylized model, we assume that  $(\theta, \phi, \varepsilon, \xi)$  are jointly normal and that all their pairwise correlations are zero with the exception of  $\text{Corr}[\theta, \phi] = \rho \neq 0$ . We write  $\sigma_{\theta|\phi}^2 := \text{Var}[\theta | \phi] = (1 - \rho^2)\sigma_\theta^2 < \sigma_\theta^2$ .

We think of  $\hat{\theta}^{\text{cl}}$  as the baseline classical statistical estimator of a quantity  $\theta$  that we seek to estimate with small MSE. In our stylized Gaussian model,  $\hat{\theta}^{\text{cl}}$  is unbiased for  $\theta$  and has noise contribution  $\xi + \varepsilon$ , so that  $\mathbb{E}[(\hat{\theta}^{\text{cl}} - \theta)^2] = \text{Var}_\theta[\hat{\theta}^{\text{cl}}] = \sigma_\xi^2 + \sigma_\varepsilon^2$ . We describe three high-level strategies used to improve the MSE of  $\hat{\theta}^{\text{cl}}$ . These strategies are not tied in any way to the stylized model; nevertheless, the stylized model enables us to give precise expressions for the risk reductions possible, see Table 1.

**Variance reduction (VR).** An important statistical idea is to improve  $\hat{\theta}^{\text{cl}}$  via obtaining further information to intercept some of its noise, say  $\xi$ , and replacing  $\hat{\theta}^{\text{cl}}$  by  $\hat{\theta}^{\text{cl}} - \xi$  which has MSE  $\sigma_\varepsilon^2$  and remains unbiased for  $\theta$ . This idea lies at the heart of approaches such as control variates in simulation [Lavenberg and Welch, 1981, Hickernell et al., 2005], variance reduction in randomized controlled experiments via covariate adjustment [Lin, 2013] and by utilizing pre-experiment data [Deng et al., 2013, CUPED], as well as model-assisted estimation in survey sampling [Cochran, 1977, Breidt and Opsomer, 2017]. It is also the idea powering PPI and related methods: the unlabeled dataset and the predictive model are used to intercept some of the noise in the classical statistical estimator  $\hat{\theta}^{\text{cl}} \triangleq \bar{Y}$ ; compare to Eq. (2) with  $\xi \triangleq \bar{Z}^f - \tilde{Z}^f$ . We refer to Ji et al. [2025] for an informative discussion of how PPI relates to traditional ideas in semi-parametric inference as in e.g., Robins et al. [1994].

Table 1: Estimator comparison in the stylized Gaussian model of Section 3.

Estimator	MSE	VR	P	CP
$\hat{\theta}^{\text{cl}}$	$\sigma_\xi^2 + \sigma_\varepsilon^2$	$\times$	$\times$	$\times$
$\hat{\theta}^{\text{cl}} - \xi$	$\sigma_\varepsilon^2$	$\checkmark$	$\times$	$\times$
$\mathbb{E}[\theta \mid \hat{\theta}^{\text{cl}}]$	$\frac{(\sigma_\xi^2 + \sigma_\varepsilon^2)\sigma_\theta^2}{(\sigma_\xi^2 + \sigma_\varepsilon^2) + \sigma_\theta^2}$	$\times$	$\checkmark$	$\times$
$\mathbb{E}[\theta \mid \hat{\theta}^{\text{cl}}, \phi]$	$\frac{(\sigma_\xi^2 + \sigma_\varepsilon^2)\sigma_{\theta \phi}^2}{(\sigma_\xi^2 + \sigma_\varepsilon^2) + \sigma_{\theta \phi}^2}$	$\times$	$\checkmark$	$\checkmark$
$\mathbb{E}[\theta \mid \hat{\theta}^{\text{cl}} - \xi]$	$\frac{\sigma_\varepsilon^2 \sigma_\theta^2}{\sigma_\varepsilon^2 + \sigma_\theta^2}$	$\checkmark$	$\checkmark$	$\times$
$\mathbb{E}[\theta \mid \hat{\theta}^{\text{cl}} - \xi, \phi]$	$\frac{\sigma_\varepsilon^2 \sigma_{\theta \phi}^2}{\sigma_\varepsilon^2 + \sigma_{\theta \phi}^2}$	$\checkmark$	$\checkmark$	$\checkmark$

VR: Variance Reduction, P: Prior Information, CP: Contextual Prior Information.

**Prior information (P) via empirical Bayes (EB).** In the Bayesian approach we seek to improve upon  $\hat{\theta}^{\text{cl}}$  by using the prior information that  $\theta \sim \mathcal{N}(0, \sigma_\theta^2)$ . The Bayes estimator,

$$\mathbb{E}[\theta \mid \hat{\theta}^{\text{cl}}] = \frac{\sigma_\theta^2}{\sigma_\xi^2 + \sigma_\varepsilon^2 + \sigma_\theta^2} \hat{\theta}^{\text{cl}},$$

reduces variance by shrinking  $\hat{\theta}^{\text{cl}}$  toward 0 (at the cost of introducing some bias). When  $\sigma_\theta^2$  is small, the MSE of  $\mathbb{E}[\theta \mid \hat{\theta}^{\text{cl}}]$  can be substantially smaller than that of  $\hat{\theta}^{\text{cl}}$ .

Now suppose that the variance of the prior,  $\sigma_\theta^2$ , is unknown but we observe data from multiple related problems generated from the same model and indexed by  $j = 1, \dots, m$ , say,  $\theta_j \stackrel{\text{iid}}{\sim} \mathcal{N}(0, \sigma_\theta^2)$  and  $\hat{\theta}_j^{\text{cl}} \stackrel{\text{iid}}{\sim} \mathcal{N}(\theta_j, \sigma_\xi^2 + \sigma_\varepsilon^2)$ . Then an EB analysis can mimic the MSE of the oracle Bayesian that has full knowledge of the prior. To wit, we can estimate  $\sigma_\theta^2$  as

$$\hat{\sigma}_\theta^2 = \left\{ \frac{1}{m-2} \sum_{j=1}^m (\hat{\theta}_j^{\text{cl}})^2 \right\} - (\sigma_\xi^2 + \sigma_\varepsilon^2),$$

and then consider a plug-in approximation of the Bayes rule,  $\hat{\theta}_j^{\text{JS}} = \mathbb{E}[\theta_j \mid \hat{\theta}_j^{\text{cl}}] := \{\hat{\sigma}_\theta^2 / (\sigma_\xi^2 + \sigma_\varepsilon^2 + \hat{\sigma}_\theta^2)\} \hat{\theta}_j^{\text{cl}}$ . The resulting estimator is the celebrated James-Stein estimator [James and Stein, 1961, Efron and Morris, 1973], whose risk is very close to the Bayes risk under the hierarchical model. The James-Stein estimator also always dominates the classical estimator under a frequentist evaluation of compound risk in (9) under the assumption that  $\hat{\theta}_j^{\text{cl}} \stackrel{\text{iid}}{\sim} \mathcal{N}(\theta_j, \sigma_\xi^2 + \sigma_\varepsilon^2)$ :

$$\mathcal{R}_m(\hat{\theta}^{\text{JS}}, \boldsymbol{\theta}) < \mathcal{R}_m(\hat{\theta}^{\text{cl}}, \boldsymbol{\theta}) \quad \text{for all } \boldsymbol{\theta} \in \mathbb{R}^m.$$

**Contextual prior information (CP) via EB.** Instead of using the same prior for each problem, we may try to sharpen the prior and increase its relevance [Efron, 2011] by using further information  $\phi$ . In the stylized example, as seen in Table 1, such an approach reduces the variance of the prior from  $\sigma_\theta^2$  to  $\sigma_{\theta|\phi}^2 < \sigma_\theta^2$  with corresponding MSE reduction of the Bayes estimator. With multiple related problems, such a strategy can be instantiated via EB shrinkage toward an informative but biased predictor [Fay III and Herriot, 1979, Green and Strawderman, 1991, Mukhopadhyay and Maiti, 2004, Kou and Yang, 2017, Rosenman et al., 2023]. The strategy of this form that is closest to our proposal is the covariate-powered EB approach of Ignatiadis and Wager [2019]. Therein (following the notation of Section 2.2), the analyst has access to classical estimators  $\bar{Y}_j$ ,  $j \in [m]$ , and problem-specific covariates  $W_j$  and seeks to shrink  $\bar{Y}_j$  toward ML models that predict  $Y_j$  from  $W_j$ . By contrast, in our setting we have observation-level covariates  $X_{ij}$  and the ML model operates on these covariates. In principle one could simultaneously use both types of covariates: problem-specific and observation-specific.

**Combined variance reduction (VR) and prior information (P).** One can shrink the variance reduced estimator  $\hat{\theta}^{\text{cl}} - \xi$  toward 0 via  $\mathbb{E}[\theta \mid \hat{\theta}^{\text{cl}} - \xi] = \{\sigma_\theta^2 / (\sigma_\varepsilon^2 + \sigma_\theta^2)\} (\hat{\theta}^{\text{cl}} - \xi)$ . In the context of PPI, variance reduction and prior information (with a more heavy-tailed prior) are used by Cortinovis

and Caron [2025] within the Frequentist-Assisted by Bayes (FAB) framework of Yu and Hoff [2018]. Cortinovis and Caron [2025] only consider a single problem and do not pursue an empirical Bayes approach.

**Combined variance reduction (VR), prior (P), and contextual prior information (CP).** Finally, in our stylized example, we can get the smallest MSE (last row of Table 1) by using both variance reduction, shrinkage, and a contextual prior. In that case, the Bayes estimator takes the form,

$$\mathbb{E}[\theta \mid \hat{\theta}^{\text{cl}} - \xi, \phi] = \frac{\sigma_{\theta|\phi}^2}{\sigma_{\varepsilon}^2 + \sigma_{\theta|\phi}^2}(\hat{\theta}^{\text{cl}} - \xi) + \frac{\sigma_{\varepsilon}^2}{\sigma_{\varepsilon}^2 + \sigma_{\theta|\phi}^2}\mathbb{E}[\theta \mid \phi]. \quad (12)$$

EB ideas can be used to mimic the estimator above and provide the starting point for our proposal that we describe next.

## 4 Prediction-Powered Adaptive Shrinkage

On a high level, PAS aims to provide a lightweight approach that outperforms both baselines in (2) and PPI/PPI++ in terms of MSE when estimating multiple means. PAS also aims at minimal modeling requirements and assumptions.

The stylized example from Section 3 serves as a guiding analogy. We seek to benefit from ML predictions in two ways: first by variance reduction (acting akin to  $\xi$  in the stylized example), and second by increasing prior relevance (acting as a proxy for  $\phi$ ). We implement both steps to adapt to the unknown data-generating process in an assumption-lean way using *within*-problem information for the first step (Section 4.1) and *across*-problem information for the second step (Section 4.2), drawing on ideas from the EB literature.

### 4.1 The Within Problem Power-Tuning Stage

Extending the notation from (4) to each problem  $j$  provides us with a class of unbiased estimators  $\hat{\theta}_{j,\lambda}^{\text{PPI}} := \bar{Y}_j + \lambda(\bar{Z}_j^f - \bar{Z}_j^f)$ ,  $\lambda \in \mathbb{R}$ . Calculating the variance gives

$$\text{Var}_{\eta_j}[\hat{\theta}_{j,\lambda}^{\text{PPI}}] = \frac{\sigma_j^2}{n_j} + \overbrace{\frac{n_j + N_j}{n_j N_j} \lambda^2 \tau_j^2 - \frac{2}{n_j} \lambda \gamma_j}^{=: \delta_j(\lambda)}.$$

Note that the classical estimator has risk  $\sigma_j^2/n_j$  and so is outperformed whenever  $\delta_j(\lambda) < 0$ . We can analytically solve for the optimal  $\lambda$ , which yields

$$\lambda_j^* := \arg \min_{\lambda} \delta_j(\lambda) = \left( \frac{N_j}{n_j + N_j} \right) \frac{\gamma_j}{\tau_j^2}, \quad (13)$$

and the Power-Tuned (PT) estimator  $\hat{\theta}_j^{\text{PT}} := \hat{\theta}_{j,\lambda_j^*}^{\text{PPI}}$  with

$$\tilde{\sigma}_j^2 := \text{Var}_{\eta_j}[\hat{\theta}_j^{\text{PT}}] = \frac{\sigma_j^2}{n_j} - \frac{N_j}{n_j(n_j + N_j)} \frac{\gamma_j^2}{\tau_j^2}. \quad (14)$$

The formulation of the above PT estimators is well understood in the single problem setting [Angelopoulos et al., 2024, Miao et al., 2024a]. In PAS, we execute this stage separately for each problem, as the optimal power-tuning parameter is data-dependent and varies case by case.

### 4.2 The Across Problem Adaptive Shrinkage Stage

The PT estimator derived in Section 4.1 already possesses many appealing properties: it is unbiased and has lower variance than both the classical estimator and vanilla PPI. However, as our setting involves working with many parallel problems together, there is the opportunity of further MSE reduction by

introducing bias in a targeted way. Concretely, based on the PT estimator obtained in Section 4.1, we consider a class of shrinkage estimators

$$\hat{\theta}_{j,\omega}^{\text{PAS}} := \omega_j \hat{\theta}_j^{\text{PT}} + (1 - \omega_j) \tilde{Z}_j^f, \quad \omega_j := \omega_j(\omega) = \frac{\omega}{\omega + \tilde{\sigma}_j^2}, \quad \hat{\theta}_\omega^{\text{PAS}} := (\hat{\theta}_{1,\omega}^{\text{PAS}}, \dots, \hat{\theta}_{m,\omega}^{\text{PAS}})^\top, \quad (15)$$

for any  $\omega \geq 0$ . The motivation is to formally match the form of the Bayes estimator with variance reduction and contextual prior information in (12) with the following (approximate) analogies:

$$\begin{aligned} \hat{\theta}^{\text{cl}} - \xi &\longleftrightarrow \hat{\theta}_j^{\text{PT}}, & \mathbb{E}[\theta \mid \phi] &\longleftrightarrow \tilde{Z}_j^f, \\ \sigma_\varepsilon^2 &\longleftrightarrow \tilde{\sigma}_j^2, & \sigma_{\theta|\phi}^2 &\longleftrightarrow \omega. \end{aligned} \quad (16)$$

The highlighted  $\omega$  is a global shrinkage parameter that acts as follows:

- (i) Fixing  $\omega$ , any problem whose PT estimator has higher variance possesses smaller  $\omega_j$  and shrinks more towards  $\tilde{Z}_j^f$ ; a smaller variance increases  $\omega_j$  and makes the final estimator closer to  $\hat{\theta}_j^{\text{PT}}$ .
- (ii) Fixing all the problems, increasing  $\omega$  has an overall effect of recovering  $\hat{\theta}_j^{\text{PT}}$  (full recovery when  $\omega \rightarrow \infty$ ), and setting  $\omega = 0$  recovers  $\tilde{Z}_j^f$ .

The above establishes the conceptual importance of  $\omega$  and if we could choose  $\omega$  in an optimal way,

$$\omega^* \in \arg \min_{\omega \geq 0} \left\{ \mathcal{R}_m \left( \hat{\theta}_\omega^{\text{PAS}}, \theta \right) \right\},$$

then the resulting estimator  $\hat{\theta}_{\omega^*}^{\text{PAS}}$  would satisfy all our desiderata. And while the above construction is not feasible as the compound risk function in (9) depends on the unknown  $\eta, \theta$ , we can make progress by pursuing a classical statistical idea: we can develop an unbiased estimate of the compound risk [Mallows, 1973, Stein, 1981, Efron, 2004] and then use that as a surrogate for tuning  $\omega$ .

To this end, we define the Correlation-aware Unbiased Risk Estimate (CURE),

$$\text{CURE} \left( \hat{\theta}_\omega^{\text{PAS}} \right) := \frac{1}{m} \sum_{j=1}^m \left[ (2\omega_j - 1) \tilde{\sigma}_j^2 + 2(1 - \omega_j) \tilde{\gamma}_j + (1 - \omega_j)^2 (\hat{\theta}_{j,\omega_j}^{\text{PT}} - \tilde{Z}_j^f)^2 \right],$$

where both the formula and our nomenclature (“correlation-aware”) highlight the fact that we must account for the potentially non-zero covariance between shrinkage source  $\hat{\theta}_j^{\text{PT}}$  and target  $\tilde{Z}_j^f$ ,

$$\tilde{\gamma}_j := \text{Cov}_{\eta_j} [\hat{\theta}_j^{\text{PT}}, \tilde{Z}_j^f] = \lambda_j^* \text{Var}_{\eta_j} [\tilde{Z}_j^f] = \frac{\gamma_j}{n_j + N_j}. \quad (17)$$

**Theorem 4.1.** *Under Assumption 2.2, CURE is an unbiased estimator of the compound risk defined in (9), that is, for all  $\omega \geq 0$  and all  $\eta$ ,*

$$\mathbb{E}_\eta \left[ \text{CURE} \left( \hat{\theta}_\omega^{\text{PAS}} \right) \right] = \mathcal{R}_m \left( \hat{\theta}_\omega^{\text{PAS}}, \theta \right).$$

See Appendices A and B.1 for the proof and motivation. With Theorem 4.1 in hand, we now have a systematic strategy of picking  $\omega$  by minimizing CURE, following the paradigm of tuning parameter selection via minimization of an unbiased risk estimate as advocated e.g., by Li [1985], Donoho and Johnstone [1995], Xie et al. [2012], Candès et al. [2013], Ignatiadis and Wager [2019]:<sup>8</sup>

$$\hat{\omega} \in \arg \min_{\omega \geq 0} \text{CURE} \left( \hat{\theta}_\omega^{\text{PAS}} \right). \quad (18)$$

Even though  $\hat{\omega}$  does not admit a closed-form expression, the one-dimensional minimization can be efficiently carried out numerically (e.g. grid search). The final PAS estimator is then given by

$$\hat{\theta}_j^{\text{PAS}} := \hat{\theta}_{j,\hat{\omega}}^{\text{PAS}} = \frac{\hat{\omega}}{\hat{\omega} + \tilde{\sigma}_j^2} \hat{\theta}_j^{\text{PT}} + \frac{\tilde{\sigma}_j^2}{\hat{\omega} + \tilde{\sigma}_j^2} \tilde{Z}_j^f.$$

<sup>8</sup>The connection to EB is the following. Xie et al. [2012] and Tibshirani and Rosset [2019] explain that James-Stein-type estimators may be derived by tuning  $\sigma_\theta^2$  (in Section 3) via minimization of Stein’s [1981] unbiased risk estimate (SURE).



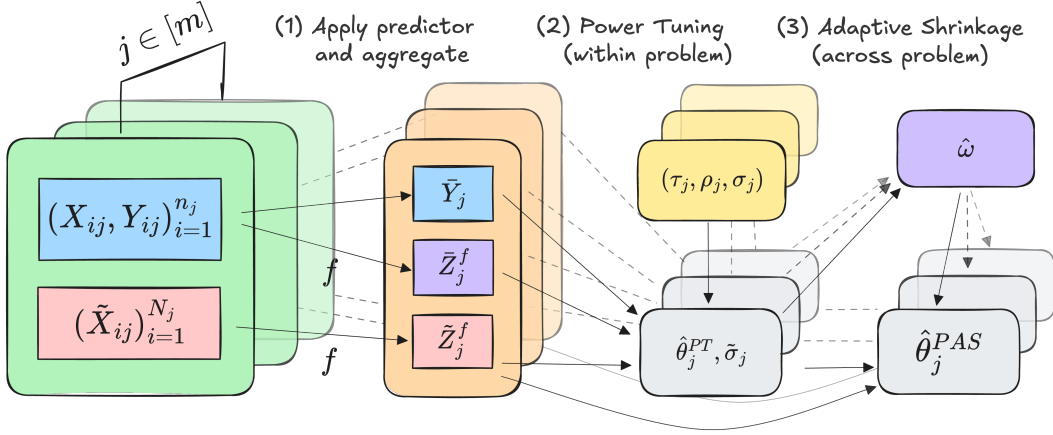


Figure 2: A flowchart illustration of the PAS method. See Algorithm 1 for a pseudo-code implementation.

---

**Algorithm 1** Prediction-Powered Adaptive Shrinkage

---

**Require:**  $(X_{ij}, Y_{ij})_{i=1}^{n_j}$ ,  $(\tilde{X}_{ij})_{i=1}^{N_j}$ ,  $\rho_j, \tau_j, \sigma_j$  for  $j \in [m]$ , predictive model  $f$

- 1: **for**  $j = 1$  to  $m$  **do**
- 2:    $\triangleright$  Step 1: Apply predictor (Eq. (1))
- 3:    $\bar{Y}_j, \bar{Z}_j^f, \tilde{Z}_j^f = \text{get\_means}((X_{ij}, Y_{ij})_{i=1}^{n_j}, (\tilde{X}_{ij})_{i=1}^{N_j}, f)$
- 4:    $\triangleright$  Step 2: Power tuning (Eq. (13))
- 5:    $\lambda_j^* = \text{get\_pt\_param}(\rho_j, \tau_j, n_j, N_j)$
- 6:    $\hat{\theta}_j^{\text{PT}} = \bar{Y}_j + \lambda_j^*(\bar{Z}_j^f - \tilde{Z}_j^f)$
- 7:    $\hat{\sigma}_j^2 = \text{get\_pt\_var}(\hat{\theta}_j^{\text{PT}}) \triangleright$  (Eq. (14))
- 8: **end for**
- 9:  $\triangleright$  Step 3: Adaptive shrinkage (Eq. (18))
- 10:  $\hat{\omega} = \text{get\_shrink\_param}(\{\hat{\theta}_j^{\text{PT}}\}_{j=1}^m, \{\bar{Z}_j^f\}_{j=1}^m, \{\hat{\sigma}_j^2\}_{j=1}^m)$
- 11: **for**  $j = 1$  to  $m$  **do**
- 12:    $\hat{\omega}_j = \hat{\omega} / (\hat{\omega} + \hat{\sigma}_j^2)$
- 13:    $\hat{\theta}_j^{\text{PAS}} = \hat{\omega}_j \hat{\theta}_j^{\text{PT}} + (1 - \hat{\omega}_j) \tilde{Z}_j^f$
- 14: **end for**
- 15: **return**  $\{\hat{\theta}_j^{\text{PAS}}\}_{j=1}^m$

---

Figure 2 visualizes the full method for constructing the PAS estimator—from applying the predictor and obtaining aggregated statistics to going through the two stages described in Section 4.1 and this section. A pseudo-code implementation is also presented in Algorithm 1.

To illustrate the flexibility and adaptivity of PAS, we briefly revisit the synthetic model in Example 2.3, whose special structure allows us to visualize how the power-tuned and adaptive shrinkage parameters vary across problems and different predictors. In Figure 3, we consider  $m = 200$  problems and two predictors: a good predictor  $f_1(x) = x^2$  and a flawed predictor  $f_2(x) = |x|$ . The model setup in (8) is such that the magnitude of  $\text{Cov}_{\eta_j}[X_j, Y_j]$  relative to  $\text{Var}_{\eta_j}[Y_j]$  is much larger for problems with  $\eta_j$  closer to the origin. Therefore, for both predictors, we see a dip in  $\lambda_j^*$  near the middle (top panel), which shows that PAS adapts to the level of difficulty of each problem when deciding how much power-tuning to apply. On the other hand (bottom panel), the overall shrinkage effect is much stronger (smaller  $\hat{\omega}_j$  for all  $j$ ) with  $f_1$  than with  $f_2$ , which demonstrates PAS’s ability to adapt to the predictor’s quality across problems—while still allowing each problem to have its own shrinkage level. Numerical results are postponed to Section 6.

## 5 Theoretical Results

In (18), we proposed selecting  $\hat{\omega}$  by optimizing an unbiased surrogate of true risk. In this section we justify this procedure theoretically. Our first result establishes that CURE approximates the true loss (whose expectation is the compound risk in (9)) uniformly in  $\omega$  as we consider more and more problems.

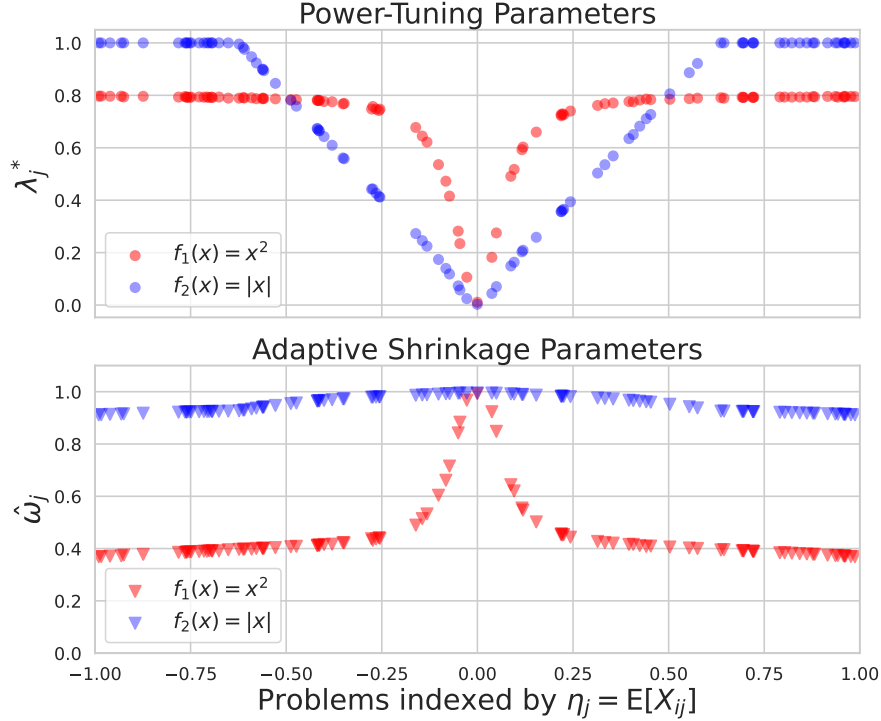


Figure 3: The power-tuned and adaptive shrinkage parameters,  $\lambda_j^*$  and  $\hat{\omega}_j$  across  $m = 200$  problems in Example 2.3. On the  $x$ -axis, we identify the problem by its  $\eta_j$  so the trend is more visible.

**Proposition 5.1.** *Suppose the datasets are generated according to Assumptions 2.1 and 2.2 and further assume that  $\mathbb{E}_{\mathbb{P}_\eta}[Y_{ij}^4] < \infty$ ,  $\mathbb{E}_{\mathbb{P}_\eta}[f(X_{ij})^4] < \infty$ . Then,*

$$\mathbb{E}_{\mathbb{P}_\eta} \left[ \sup_{\omega \geq 0} \left| \text{CURE}(\hat{\theta}_\omega^{\text{PAS}}) - \ell_m(\hat{\theta}_\omega^{\text{PAS}}, \theta) \right| \right] = o(1),$$

where  $o(1)$  denotes a term that converges to 0 as  $m \rightarrow \infty$ .

A principal consequence of Proposition 5.1 is that PAS with the data-driven choice of  $\hat{\omega}$  in (18) has asymptotically smaller Bayes MSE (defined in (11)) than any of the estimators in (15), i.e. it has smaller MSE than both baselines in (2) as well as the PPI and PT estimators.

**Theorem 5.2.** *Under the assumptions of Proposition 5.1,*

$$\mathcal{B}_m^{\mathbb{P}_\eta}(\hat{\theta}_{\hat{\omega}}^{\text{PAS}}) \leq \inf_{\omega \geq 0} \left\{ \mathcal{B}_m^{\mathbb{P}_\eta}(\hat{\theta}_\omega^{\text{PAS}}) \right\} + o(1) \text{ as } m \rightarrow \infty,$$

and so

$$\mathcal{B}_m^{\mathbb{P}_\eta}(\hat{\theta}_{\hat{\omega}}^{\text{PAS}}) \leq \min \left\{ \mathcal{B}_m^{\mathbb{P}_\eta}(\tilde{\mathbf{Z}}^f), \mathcal{B}_m^{\mathbb{P}_\eta}(\hat{\theta}^{\text{PT}}) \right\} + o(1).$$

Our next proposition connects Theorem 5.2 with the lowest possible MSE in the stylized Gaussian example of Section 3 (last row of Table 1).

**Proposition 5.3.** *In addition to the assumptions of Proposition 5.1, further assume that  $N_j = \infty$  and that there exist  $n \in \mathbb{N}$ ,  $\tilde{\sigma}^2 > 0$  such that  $n_j = n$  and  $\tilde{\sigma}_j^2 = \tilde{\sigma}^2$  for all  $j$  almost surely. Let  $\beta^2 := \mathbb{E}_{\mathbb{P}_\eta}[(\tilde{Z}_j^f - \theta_j)^2]$  (which does not depend on  $j$  as we are integrating over  $\mathbb{P}_\eta$ ). Then, as  $m \rightarrow \infty$ ,*

$$\mathcal{B}_m^{\mathbb{P}_\eta}(\hat{\theta}_{\hat{\omega}}^{\text{PAS}}) \leq \frac{\tilde{\sigma}^2 \beta^2}{\tilde{\sigma}^2 + \beta^2} + o(1).$$

To interpret the result, it is instructive to compare the asymptotic upper bound on the MSE of PAS with the MSE in the last line of Table 1, i.e., with  $(\sigma_\varepsilon^2 \sigma_{\theta|\phi}^2)/(\sigma_\varepsilon^2 + \sigma_{\theta|\phi}^2)$ . Observe that  $\tilde{\sigma}^2$  plays the role

of  $\sigma_\varepsilon^2$  (as already anticipated in (16)) which is smaller than the variance of the classical estimator (due to power tuning). Meanwhile,  $\beta^2$  plays the role of  $\sigma_{\theta|\phi}^2$ . If the baseline  $\tilde{Z}_j^f$  that is the mean of the ML predictions on the unlabeled datasets is doing a good job of predicting  $\theta_j$ , then  $\beta^2$  will be small, and so PAS may have MSE substantially smaller than that of PT. On the other hand, even if  $\beta^2$  is large (that is, even if the ML model is very biased), PAS asymptotically still has MSE less or equal than  $\tilde{\sigma}^2$ , the MSE of PT. We emphasize that the role of Proposition 5.3 is to provide intuition at the expense of strong assumptions. By contrast, the statement of Theorem 5.2 does not restrict heterogeneity (e.g., heteroscedasticity) across problems and allows for varying, finite unlabeled and labeled sample sizes.

## 6 Experiments

We apply the proposed PAS estimator and conduct extensive experiments in both the synthetic model proposed in Example 2.3 and two real-world datasets.

**Baselines.** We compare the PAS estimator against both classical and modern baseline estimators:

- (i.) the classical estimator;
- (ii.) prediction mean on unlabeled data;
- (iii.) the vanilla PPI estimator [Angelopoulos et al., 2023];
- (iv.) the PT estimator [Angelopoulos et al., 2024, PPI++];
- (v.) the “shrink-classical” estimator that directly shrinks the classical estimator toward the prediction mean;
- (vi.) the “shrink-average” estimator that shrinks  $\hat{\theta}_j^{\text{PT}}$  toward the PT group mean across all problems,  $\bar{\theta}^{\text{PT}} := m^{-1} \sum_j \hat{\theta}_j^{\text{PT}}$ .

See Appendix C for detailed formulations and implementations for (v.) & (vi.) (the latter of which is inspired by the SURE-grand mean estimator of Xie et al. [2012]). The comparisons with (iv.) and (v.) also directly serve as ablation studies of the two stages in constructing the PAS estimator.

**Metrics.** We report the mean squared error (MSE) ( $\pm 1$  standard error) of each estimator  $\hat{\theta}$  by averaging  $\frac{1}{m} \sum_{j=1}^m (\hat{\theta}_j - \theta_j)^2$  across  $K = 200$  Monte Carlo replicates. In the synthetic model, we sample  $\eta_j$  (and thus  $\theta_j$ ) from the known prior  $\mathbb{P}_\eta$ . For the real-world datasets, since  $\mathbb{P}_\eta$  is unknown, we follow the standard evaluation strategy in the PPI literature: we start with a large labeled dataset and use it to compute a pseudo-ground truth for each mean  $\theta_j$ . Then in each Monte Carlo replicate, we randomly split the data points of each problem into labeled/unlabeled partitions (where we choose a 20/80 split ratio). We provide more details on the benchmarking procedure for the MSE in Appendix D.

For real-world datasets, we introduce a second metric to assess whether improvements in MSE are driven by a few difficult problems rather than consistent performance gains: the percentage of problems improved relative to the classical estimator. This metric is defined as

$$\% \text{ Improved } \uparrow := \frac{1}{m} \sum_{j=1}^m \mathbf{1} \left[ (\hat{\theta}_j - \theta_j)^2 < (\hat{\theta}_j^{\text{Classical}} - \theta_j)^2 \right] \times (100\%).$$

Larger values of this metric are preferable.

### 6.1 Synthetic Model

This is the synthetic model from Example 2.3, where we choose  $m = 200$ ,  $n_j = 20$ , and  $N_j = 80$  for all  $j$ . Since we have already visualized the model and the parameters of the PAS estimator in previous sections, we simply report the numerical results (for the good predictor  $f_1$  and the flawed predictor  $f_2$ ) in Table 2.

For both predictors, we see that PAS outperforms all the baselines. With a good predictor  $f_1$ , both the prediction mean and the shrinkage estimator closely track PAS; in contrast, the PPI and PT

Table 2: MSE ( $\pm$  standard error) of different estimators under the synthetic model with predictors  $f_1(x) = x^2$ , respectively  $f_2(x) = |x|$ .

Estimator	MSE $f_1$ ( $\times 10^{-3}$ )	MSE $f_2$ ( $\times 10^{-3}$ )
Classical	3.142 $\pm$ 0.033	3.142 $\pm$ 0.033
Prediction Avg	0.273 $\pm$ 0.004	34.335 $\pm$ 0.147
PPI	2.689 $\pm$ 0.027	2.756 $\pm$ 0.027
PT	2.642 $\pm$ 0.027	2.659 $\pm$ 0.026
Shrink Classical	0.273 $\pm$ 0.003	3.817 $\pm$ 0.042
Shrink Avg	2.486 $\pm$ 0.026	2.575 $\pm$ 0.026
<b>PAS (ours)</b>	<b>0.272 <math>\pm</math> 0.003</b>	<b>2.496 <math>\pm</math> 0.025</b>

Table 3: Results aggregated over  $K = 200$  replicates on the Amazon review dataset with BERT-base and BERT-tuned predictors. Metrics are reported with  $\pm 1$  standard error.

Estimator	Amazon (base $f$ )		Amazon (tuned $f$ )	
	MSE ( $\times 10^{-3}$ )	% Improved $\uparrow$	MSE ( $\times 10^{-3}$ )	% Improved $\uparrow$
Classical	24.305 $\pm$ 0.189	baseline	24.305 $\pm$ 0.189	baseline
Prediction Avg	41.332 $\pm$ 0.050	30.7 $\pm$ 0.2	3.945 $\pm$ 0.011	75.4 $\pm$ 0.2
PPI	11.063 $\pm$ 0.085	62.4 $\pm$ 0.2	7.565 $\pm$ 0.066	70.4 $\pm$ 0.2
PT	10.633 $\pm$ 0.089	70.3 $\pm$ 0.2	6.289 $\pm$ 0.050	76.0 $\pm$ 0.2
Shrink Classical	15.995 $\pm$ 0.121	56.4 $\pm$ 0.3	3.828 $\pm$ 0.039	78.9 $\pm$ 0.2
Shrink Avg	9.276 $\pm$ 0.078	70.4 $\pm$ 0.2	6.280 $\pm$ 0.058	77.1 $\pm$ 0.2
<b>PAS (ours)</b>	<b>8.517 <math>\pm</math> 0.071</b>	<b>71.4 <math>\pm</math> 0.2</b>	<b>3.287 <math>\pm</math> 0.024</b>	<b>80.8 <math>\pm</math> 0.2</b>

estimators fail to fully leverage the accurate predictions, as their design enforces unbiasedness. The situation reverses for the less reliable predictor  $f_2$ : the prediction mean and the shrinkage estimator have high MSE, while estimators with built-in de-biasing mechanisms demonstrate greater resilience. PAS adapts effectively across these extremes, making it a robust choice for a wide range of problems and predictors.

## 6.2 Real-World Datasets

We next evaluate PAS on two large-scale real-world datasets, highlighting its ability to leverage state-of-the-art deep learning models in different settings. We include only the essential setup below and defer additional data and model details (e.g., hyper-parameters, preprocessing) to Appendix D.

Table 4: Results aggregated over  $K = 200$  replicates on the Galaxy dataset with ResNet50 predictor. Metrics are reported with  $\pm 1$  standard error.

Estimator	Galaxy	
	MSE ( $\times 10^{-3}$ )	% Improved $\uparrow$
Classical	2.073 $\pm$ 0.028	baseline
Prediction Avg	7.195 $\pm$ 0.008	17.0 $\pm$ 0.2
PPI	1.149 $\pm$ 0.017	59.4 $\pm$ 0.3
PT	1.026 $\pm$ 0.015	67.7 $\pm$ 0.3
Shrink Classical	1.522 $\pm$ 0.016	48.8 $\pm$ 0.4
Shrink Avg	0.976 $\pm$ 0.014	<b>68.9 <math>\pm</math> 0.3</b>
<b>PAS (ours)</b>	<b>0.893 <math>\pm</math> 0.011</b>	67.3 $\pm$ 0.4

**Amazon Review Ratings** [SNAP, 2014]. Many commercial and scientific studies involve collecting a large corpus of text and estimating an average score (rating, polarity, etc.) from it. A practitioner would often combine limited human annotations with massive automatic evaluations from ML models [Tyser et al., 2024, Baly et al., 2020]. To emulate this setup, we consider mean rating estimation problems using the Amazon Fine Food Review dataset from Kaggle, where we artificially hide the labels in a random subset of the full data to serve as the unlabeled partition. Concretely, we estimate the average rating for the top  $m = 200$  products with the most reviews (from  $\sim 200$  to  $\sim 900$ ). For the  $i$ -th review of the  $j$ -th product, the covariate  $X_{ij}$  consists of the review’s title and text concatenated, while the outcome  $Y_{ij}$  is the star rating in  $\{1, \dots, 5\}$ . We employ two black-box predictors: (1) **BERT-base**, a language model without fine-tuning [Devlin, 2018] and (2) **BERT-tuned** which is the same model but fine-tuned on a held-out set of reviews from other products. Neither of these models have seen the reviews for the 200 products during training.

**Spiral Galaxy Fractions** [Willett et al., 2013]. The Galaxy Zoo 2 project contains the classification results of galaxy images from the Sloan Digital Sky Survey [York et al., 2000, SDSS]. We are interested in estimating the fraction of galaxies that are classified as “spiral,” i.e., have at least one spiral arm. The covariates  $X_{ij}$  in this applications are images (we provide some examples in Figure 6 of the appendix). Existing PPI papers have focused on estimating the overall fraction; we demonstrate how this dataset’s metadata structure enables compound estimation of spiral fractions across distinct galaxy subgroups. We first use a pre-defined partition of the galaxies into 122 subgroups that is based on the metadata attribute REDSHIFT. Second, we estimate the fraction of spiral galaxies in all of the galaxy subgroups simultaneously. For the predictor, we train a **ResNet50** convolutional neural network on a held-out set with around 50k images.

For both datasets, we randomly split the data for each problem (a food product or galaxy subgroup) into a labeled and unlabeled partition with a 20/80 ratio. We repeat the random splitting  $K = 200$  times and report metrics averaged over all splits. Results are displayed in Table 3, and here is a brief summary:

- **Amazon Review:** similar to the trend in the synthetic model, the more accurate **BERT-tuned** model enables stronger shrinkage for PAS while the biased **BERT-base** predictions necessitate less shrinkage. Our PAS estimator adapts to both predictors and outperforms other baselines. PAS has the lowest MSE without sacrificing performance on our second metric.
- **Galaxy Zoo 2:** the predictions from **ResNet50** are suboptimal, so the variance-reduction from power tuning dominates any benefit from shrinkage. PAS achieves the lowest MSE among all estimators, and improves individual estimates at a level on par with the shrink-towards-mean estimator.

In Figure 4, we visualize the PAS and PT estimators against the pseudo-ground truth  $\theta_j$  for each problem in the Galaxy Zoo and Amazon Review (with **BERT-tuned**) datasets. With the quantitative results obtained above, it is not surprising to see PAS estimators being closer to the  $45^\circ$  line of perfect estimation. More importantly, the spread of pseudo-ground truth  $\theta_j$  suggests that there is substantial heterogeneity (in outcome means) across different problems, justifying the stratification procedure and the compound mean estimation setting.

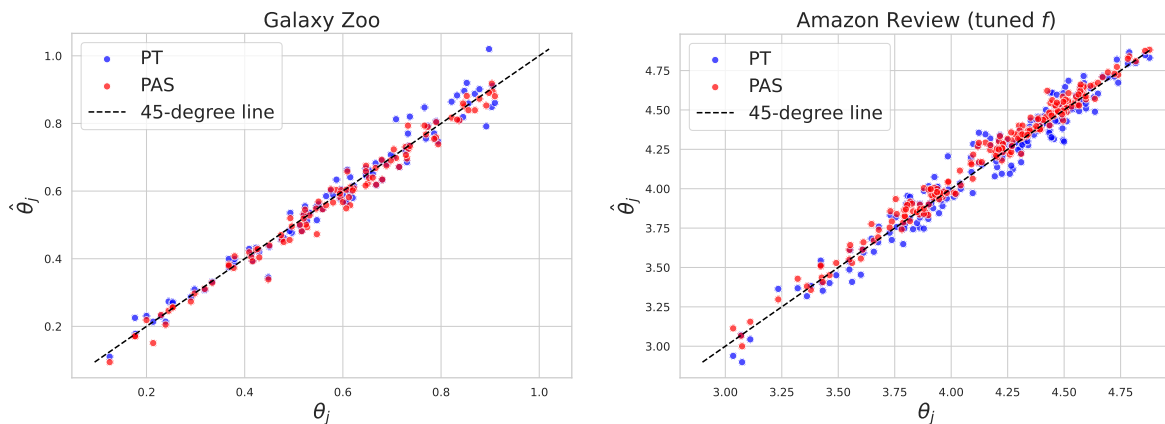


Figure 4: Comparison between the PAS and PT (PPI++) estimators for each problem in the Galaxy Zoo and Amazon Review (with BERT-tuned) datasets. The dashed 45° line indicates perfect estimation against the pseudo-ground truth  $\theta_j$ .

## 7 Conclusion

This paper introduces PAS, a novel method for compound mean estimation that effectively combines PPI and EB principles. We motivate the problem through the lens of variance reduction and contextual prior information—then demonstrate how PAS achieves both goals, in theory and in practice. Our paper differs from many other PPI-related works in its focus on estimation, so a natural next step is to develop average coverage controlling intervals for the means centered around PAS. To this end, it may be fruitful to build on the robust empirical Bayes confidence intervals of [Armstrong et al. \[2022\]](#). Modern scientific inquiries increasingly demand the simultaneous analysis of multiple related problems. The framework developed in this paper—combining empirical Bayes principles with machine learning predictions—represents a promising direction for such settings.

## References

- A. N. Angelopoulos, S. Bates, C. Fannjiang, M. I. Jordan, and T. Zrníc. Prediction-powered inference. *Science*, 382(6671):669–674, 2023.
- A. N. Angelopoulos, J. C. Duchi, and T. Zrníc. PPI++: Efficient Prediction-Powered Inference. *arXiv preprint*, arXiv:2311.01453, 2024.
- T. B. Armstrong, M. Kolesár, and M. Plagborg-Møller. Robust empirical Bayes confidence intervals. *Econometrica*, 90(6):2567–2602, 2022.
- R. Baly, G. Da San Martino, J. Glass, and P. Nakov. We can detect your bias: Predicting the political ideology of news articles. In *Proceedings of the 2020 Conference on Empirical Methods in Natural Language Processing (EMNLP)*, pages 4982–4991. Association for Computational Linguistics, 2020.
- F. J. Breidt and J. D. Opsomer. Model-assisted survey estimation with modern prediction techniques. *Statistical Science*, 32(2), 2017.
- E. J. Candès, C. A. Sing-Long, and J. D. Trzasko. Unbiased risk estimates for singular value thresholding and spectral estimators. *IEEE Transactions on Signal Processing*, 61(19):4643–4657, 2013.
- W. G. Cochran. *Sampling Techniques*. Wiley Series in Probability and Mathematical Statistics. John Wiley & Sons, New York, 3d ed edition, 1977.
- S. Cortinovis and F. Caron. FAB-PPI: Frequentist, Assisted by Bayes, Prediction-Powered Inference. *arXiv preprint*, arXiv:2502.02363, 2025.

- A. Deng, Y. Xu, R. Kohavi, and T. Walker. Improving the sensitivity of online controlled experiments by utilizing pre-experiment data. In *Proceedings of the Sixth ACM International Conference on Web Search and Data Mining*, pages 123–132, Rome Italy, 2013. ACM.
- J. Deng, W. Dong, R. Socher, L.-J. Li, K. Li, and L. Fei-Fei. Imagenet: A large-scale hierarchical image database. In *2009 IEEE Conference on Computer Vision and Pattern Recognition*, pages 248–255. Ieee, 2009.
- J. Devlin. Bert: Pre-training of deep bidirectional transformers for language understanding. *arXiv preprint*, arXiv:1810.04805, 2018.
- D. L. Donoho and I. M. Johnstone. Adapting to unknown smoothness via wavelet shrinkage. *Journal of the American Statistical Association*, 90(432):1200–1224, 1995.
- R. Durrett. *Probability: Theory and Examples*, volume 49 of *Cambridge Series in Statistical and Probabilistic Mathematics*. Cambridge University Press, 5th edition, 2019.
- B. Efron. The estimation of prediction error: Covariance penalties and cross-validation. *Journal of the American Statistical Association*, 99(467):619–632, 2004.
- B. Efron. *Large-Scale Inference: Empirical Bayes Methods for Estimation, Testing, and Prediction*. Institute of Mathematical Statistics Monographs. Cambridge University Press, Cambridge, 2010.
- B. Efron. Tweedie’s formula and selection bias. *Journal of the American Statistical Association*, 106(496):1602–1614, 2011.
- B. Efron and C. Morris. Stein’s estimation rule and its competitors—an empirical Bayes approach. *Journal of the American Statistical Association*, 68(341):117–130, 1973.
- R. E. Fay III and R. A. Herriot. Estimates of income for small places: An application of James-Stein procedures to census data. *Journal of the American Statistical Association*, 74(366a):269–277, 1979.
- A. Fisch, J. Maynez, R. A. Hofer, B. Dhingra, A. Globerson, and W. W. Cohen. Stratified prediction-powered inference for hybrid language model evaluation. *arXiv preprint*, arXiv:2406.04291, 2024.
- E. J. Green and W. E. Strawderman. A James-Stein type estimator for combining unbiased and possibly biased estimators. *Journal of the American Statistical Association*, 86(416):1001–1006, 1991.
- R. E. Hart, S. P. Bamford, K. W. Willett, K. L. Masters, C. Cardamone, C. J. Lintott, R. J. Mackay, R. C. Nichol, C. K. Rosslove, B. D. Simmons, and R. J. Smethurst. Galaxy Zoo: comparing the demographics of spiral arm number and a new method for correcting redshift bias. *Monthly Notices of the Royal Astronomical Society*, 461(4):3663–3682, Oct. 2016.
- K. He, X. Zhang, S. Ren, and J. Sun. Deep residual learning for image recognition. In *Proceedings of the IEEE Conference on Computer Vision and Pattern Recognition*, pages 770–778, 2016.
- K. He, X. Chen, S. Xie, Y. Li, P. Dollár, and R. Girshick. Masked autoencoders are scalable vision learners. In *Proceedings of the IEEE/CVF Conference on Computer Vision and Pattern Recognition*, pages 16000–16009, 2022.
- F. J. Hickernell, C. Lemieux, and A. B. Owen. Control variates for Quasi-Monte Carlo. *Statistical Science*, 20(1):1–31, 2005.
- N. Ignatiadis and S. Wager. Covariate-powered empirical Bayes estimation. In *Advances in Neural Information Processing Systems*, volume 32, 2019.
- N. Ignatiadis, S. Saha, D. L. Sun, and O. Muralidharan. Empirical Bayes mean estimation with nonparametric errors via order statistic regression on replicated data. *Journal of the American Statistical Association*, 118(542):987–999, 2023.
- W. James and C. Stein. Estimation with quadratic loss. In *Proceedings of the Fourth Berkeley Symposium on Mathematical Statistics and Probability*, volume 1, pages 361–379, 1961.

- W. Ji, L. Lei, and T. Zrnic. Predictions as surrogates: Revisiting surrogate outcomes in the age of AI. *arXiv preprint*, arXiv:2501.09731, 2025.
- W. Jiang and C.-H. Zhang. General maximum likelihood empirical Bayes estimation of normal means. *The Annals of Statistics*, 37(4):1647–1684, 2009.
- D. P. Kingma. Adam: A method for stochastic optimization. *arXiv preprint*, arXiv:1412.6980, 2014.
- S. C. Kou and J. J. Yang. Optimal shrinkage estimation in heteroscedastic hierarchical linear models. In S. E. Ahmed, editor, *Big and Complex Data Analysis*, pages 249–284. Springer International Publishing, Cham, 2017.
- S. S. Lavenberg and P. D. Welch. A perspective on the use of control variables to increase the efficiency of Monte Carlo simulations. *Management Science*, 27(3):322–335, 1981.
- K.-C. Li. From Stein’s Unbiased Risk Estimates to the method of Generalized Cross Validation. *The Annals of Statistics*, 13(4):1352–1377, 1985.
- F. Liang, S. Mukherjee, and M. West. The use of unlabeled data in predictive modeling. *Statistical Science*, 22(2):189–205, 2007.
- J. Y.-Y. Lin, S.-M. Liao, H.-J. Huang, W.-T. Kuo, and O. H.-M. Ou. Galaxy morphological classification with efficient vision transformer. *arXiv preprint*, arXiv:2110.01024, 2021.
- W. Lin. Agnostic notes on regression adjustments to experimental data: Reexamining Freedman’s critique. *The Annals of Applied Statistics*, 7(1):295–318, 2013.
- C. L. Mallows. Some comments on  $C_P$ . *Technometrics*, 15(4):661, 1973.
- J. Miao, X. Miao, Y. Wu, J. Zhao, and Q. Lu. Assumption-lean and data-adaptive post-prediction inference. *arXiv preprint*, arXiv:2311.14220, 2024a.
- J. Miao, Y. Wu, Z. Sun, X. Miao, T. Lu, J. Zhao, and Q. Lu. Valid inference for machine learning-assisted genome-wide association studies. *Nature Genetics*, pages 1–9, 2024b.
- P. Mukhopadhyay and T. Maiti. Two stage non-parametric approach for small area estimation. *Proceedings of ASA Section on Survey Research Methods*, hal, pages 4058–4065, 2004.
- P. B. Nair and R. G. Abraham. On the fraction of barred spiral galaxies. *The Astrophysical Journal Letters*, 714(2):L260, 2010.
- NLP Town. bert-base-multilingual-uncased-sentiment (revision edd66ab), 2023. URL <https://huggingface.co/nlptown/bert-base-multilingual-uncased-sentiment>.
- G. Penedo, H. Kydlíček, L. B. allal, A. Lozhkov, M. Mitchell, C. Raffel, L. V. Werra, and T. Wolf. The fineweb datasets: Decanting the web for the finest text data at scale. In *The Thirty-eight Conference on Neural Information Processing Systems Datasets and Benchmarks Track*, 2024.
- A. Radford, J. Wu, R. Child, D. Luan, D. Amodei, I. Sutskever, et al. Language models are unsupervised multitask learners. *OpenAI blog*, 1(8):9, 2019.
- H. Robbins. Asymptotically subminimax solutions of compound statistical decision problems. In *Proceedings of the Second Berkeley Symposium on Mathematical Statistics and Probability*, volume 2, pages 131–149. University of California Press, 1951.
- H. Robbins. An empirical Bayes approach to statistics. In *Proceedings of the Third Berkeley Symposium on Mathematical Statistics and Probability, Volume 1: Contributions to the Theory of Statistics*, pages 157–163. The Regents of the University of California, 1956.
- J. M. Robins, A. Rotnitzky, and L. P. Zhao. Estimation of regression coefficients when some regressors are not always observed. *Journal of the American Statistical Association*, 89(427):846–866, 1994.
- E. T. Rosenman, G. Basse, A. B. Owen, and M. Baiocchi. Combining observational and experimental datasets using shrinkage estimators. *Biometrics*, page biom.13827, 2023.



- SNAP. Amazon Fine Food Reviews (Stanford network analysis project). Kaggle Dataset, 2014. URL <https://www.kaggle.com/datasets/snap/amazon-fine-food-reviews/data>. Accessed: 2024-01-01.
- J. A. Soloff, A. Guntuboyina, and B. Sen. Multivariate, heteroscedastic empirical Bayes via nonparametric maximum likelihood. *Journal of the Royal Statistical Society Series B: Statistical Methodology*, page qkae040, 2024.
- C. M. Stein. Estimation of the mean of a multivariate normal distribution. *The Annals of Statistics*, pages 1135–1151, 1981.
- R. J. Tibshirani and S. Rosset. Excess optimism: How biased is the apparent error of an estimator tuned by SURE? *Journal of the American Statistical Association*, 114(526):697–712, 2019.
- K. Tyser, B. Segev, G. Longhitano, X.-Y. Zhang, Z. Meeks, J. Lee, U. Garg, N. Belsten, A. Shporer, M. Udell, et al. AI-driven review systems: evaluating LLMs in scalable and bias-aware academic reviews. *arXiv preprint arXiv:2408.10365*, 2024.
- S. Wang, T. H. McCormick, and J. T. Leek. Methods for correcting inference based on outcomes predicted by machine learning. *Proceedings of the National Academy of Sciences*, 117(48):30266–30275, 2020.
- K. W. Willett, C. J. Lintott, S. P. Bamford, K. L. Masters, B. D. Simmons, K. R. Casteels, E. M. Edmondson, L. F. Fortson, S. Kaviraj, W. C. Keel, et al. Galaxy Zoo 2: detailed morphological classifications for 304 122 galaxies from the Sloan Digital Sky Survey. *Monthly Notices of the Royal Astronomical Society*, 435(4):2835–2860, 2013.
- T. Wolf. Huggingface’s transformers: State-of-the-art natural language processing. *arXiv preprint*, arXiv:1910.03771, 2019.
- X. Xie, S. Kou, and L. D. Brown. SURE estimates for a heteroscedastic hierarchical model. *Journal of the American Statistical Association*, 107(500):1465–1479, 2012.
- D. G. York, J. Adelman, J. E. Anderson Jr, S. F. Anderson, J. Annis, N. A. Bahcall, J. Bakken, R. Barkhouser, S. Bastian, E. Berman, et al. The sloan digital sky survey: Technical summary. *The Astronomical Journal*, 120(3):1579, 2000.
- C. Yu and P. D. Hoff. Adaptive multigroup confidence intervals with constant coverage. *Biometrika*, 105(2):319–335, 2018.
- T. Zrnic. A Note on the prediction-powered bootstrap. *arXiv preprint*, arXiv:2405.18379, 2025.
- T. Zrnic and E. J. Candès. Cross-prediction-powered inference. *Proceedings of the National Academy of Sciences*, 121(15):e2322083121, 2024.

## ♣ Appendix: Table of Contents

- [A. The Correlation-Aware Unbiased Risk Estimate](#) .....Page 18
- [B. Proofs of Theoretical Results](#) .....Page 19
- [C. Baseline Shrinkage Estimators](#) .....Page 25
- [D. Experiment Details](#) .....Page 27

### A The Correlation-Aware Unbiased Risk Estimate

**Theorem A.1.** *Let  $X, Y$  be two random variables satisfying  $\mathbb{E}_\theta[X] = \theta$ ,  $\text{Var}_\theta[X] = \sigma^2$ ,  $\text{Cov}_\theta[X, Y] = \gamma$ , and the second moment of  $Y$  exists.<sup>9</sup> Consider estimating  $\theta$  with the shrinkage estimator  $\hat{\theta}_c = cX + (1 - c)Y$  with  $c \in [0, 1]$ . Assuming that  $\sigma^2$  and  $\gamma$  are known, the following estimator*

$$\text{CURE}(\hat{\theta}_c) := (2c - 1)\sigma^2 + 2(1 - c)\gamma + \{(1 - c)(X - Y)\}^2, \quad (19)$$

*defined as the Correlation-aware Unbiased Risk Estimate, is an unbiased estimator for the risk of  $\hat{\theta}_c$  under quadratic loss. That is, letting  $R(\hat{\theta}_c, \theta) := \mathbb{E}_\theta[(\hat{\theta}_c - \theta)^2]$ , it holds that:*

$$\mathbb{E}_\theta[\text{CURE}(\hat{\theta}_c)] = R(\hat{\theta}_c, \theta).$$

*Proof.* First, expand the risk:

$$\begin{aligned} R(\hat{\theta}_c, \theta) &= \mathbb{E}_\theta[(\hat{\theta}_c - \theta)^2] = \mathbb{E}_\theta[(cX + (1 - c)Y - \theta)^2] \\ &= \text{Var}_\theta[cX + (1 - c)Y] + (\mathbb{E}_\theta[cX + (1 - c)Y] - \theta)^2 \\ &= c^2\sigma^2 + (1 - c)^2\text{Var}_\theta[Y] + 2c(1 - c)\gamma + [(1 - c)(\mathbb{E}_\theta[Y] - \theta)]^2. \end{aligned}$$

Then, taking the expectation of  $\text{CURE}(\hat{\theta}_c)$ :

$$\mathbb{E}_\theta[\text{CURE}(\hat{\theta}_c)] = \underbrace{(2c - 1)\sigma^2 + 2(1 - c)\gamma}_{\text{I}} + \mathbb{E}_\theta[\{(1 - c)(X - Y)\}^2], \quad (20)$$

where the last term is

$$\begin{aligned} \mathbb{E}_\theta[\{(1 - c)(X - Y)\}^2] &= (1 - c)^2 [(\mathbb{E}_\theta[X - Y])^2 + \text{Var}_\theta[X - Y]] \\ &= (1 - c)^2 [(\mathbb{E}_\theta[Y] - \theta)^2 + \sigma^2 + \text{Var}_\theta[Y] - 2\gamma] \\ &= [(1 - c)(\mathbb{E}_\theta[Y] - \theta)]^2 + \underbrace{(1 - c)^2(\sigma^2 + \text{Var}_\theta[Y] - 2\gamma)}_{\text{II}}. \end{aligned}$$

With a little algebra, we observe

$$\begin{aligned} \text{I} + \text{II} &= (2c - 1)\sigma^2 + 2(1 - c)\gamma + (1 - c)^2(\sigma^2 + \text{Var}_\theta[Y] - 2\gamma) \\ &= c^2\sigma^2 + (1 - c)^2\text{Var}_\theta[Y] + 2c(1 - c)\gamma. \end{aligned}$$

Thus, a term-by-term matching confirms  $\mathbb{E}_\theta[\text{CURE}(\hat{\theta}_c)] = R(\hat{\theta}_c, \theta)$ . □

**Remark A.2** (Connection to SURE). Stein's Unbiased Risk Estimate (SURE) was proposed in Charles Stein's seminal work [1981] to study the quadratic risk in Gaussian sequence models. As a simple special case of SURE, let  $Z \sim \mathcal{N}(\theta, \sigma^2)$  and let  $h : \mathbb{R} \rightarrow \mathbb{R}$  be an absolutely continuous function and  $\mathbb{E}_\theta[|h'(Z)|] < \infty$ , then SURE is defined as

$$\text{SURE}(h) := (h(Z) - Z)^2 + 2\sigma^2 h'(Z) - \sigma^2,$$

---

<sup>9</sup>We redefine certain variables for generality of this result beyond the setting in Assumption 2.2. In this theorem,  $\theta$  plays the role of  $\eta$  in the main text, i.e. all the other parameters are deterministic given  $\theta$ .

with the property that  $\mathbb{E}_\theta[\text{SURE}(h)] = R(h(Z), \theta) = \mathbb{E}_\theta[(h(Z) - \theta)^2]$ . A proof of this argument relies on Stein's lemma, an identity specific to Gaussian random variables [Stein \[1981\]](#). Now consider the specific linear shrinkage estimator  $h_c(Z) := cZ + (1 - c)Y$ , with  $c \in [0, 1]$  and  $Y \in \mathbb{R}$  being fixed (that is,  $Y$  is a constant, or  $Y$  is independent of  $Z$  and we condition on  $Y$ ). Then SURE takes the following form:

$$\begin{aligned} \text{SURE}(h_c) &= (h_c(Z) - Z)^2 + 2\sigma^2 h'_c(Z) - \sigma^2 \\ &= (cZ + (1 - c)Y - Z)^2 + 2c\sigma^2 - \sigma^2 \\ &= [(1 - c)(Y - Z)]^2 + (2c - 1)\sigma^2 \\ &\stackrel{(\star)}{=} \text{CURE}(h_c(Z)), \end{aligned}$$

where in  $(\star)$  we used the fact that in this case (with  $Y$  fixed or  $Y$  independent of  $Z$ ), it holds that  $\gamma = 0$  so that the definition of CURE in [\(19\)](#) simplifies. This explains how CURE defined in [A.1](#) is connected to SURE.

We make one last remark: The derivation of SURE itself requires Gaussianity. However, for linear shrinkage rules as  $h_c(Z)$ , SURE only depends on the first two moments of the distribution of  $Z$  and thus is an unbiased estimator of quadratic risk under substantial generality as long as  $\mathbb{E}_\theta[Z] = \theta$  and  $\text{Var}_\theta[Z] = \sigma^2$ . This remark has been made by previous authors, e.g., [Kou and Yang \[2017\]](#), [Ignatiadis and Wager \[2019\]](#) and is important for the assumption-lean validity of PAS.

## B Proofs of Theoretical Results

### B.1 Proof of Theorem. 4.1

For each problem  $j \in [m]$ , we are shrinking the PT estimator  $\hat{\theta}_j^{\text{PT}}$  obtained from the first stage towards  $\tilde{Z}_j^f$ , the prediction mean on the unlabeled data. Conditioning on  $\eta_j$ , we denote

$$\begin{aligned} \tilde{\sigma}_j^2 &:= \text{Var}_{\eta_j} \left[ \hat{\theta}_j^{\text{PT}} \right] = \text{Var}_{\eta_j} \left[ \hat{\theta}_{j, \lambda_j^*}^{\text{PPI}} \right], \\ \tilde{\gamma}_j &:= \text{Cov}_{\eta_j} \left[ \hat{\theta}_j^{\text{PT}}, \tilde{Z}_j^f \right] = \lambda_j^* \text{Var}_{\eta_j} \left[ \tilde{Z}_j^f \right], \end{aligned}$$

where all the first and second moments of  $\hat{\theta}_j^{\text{PT}}$  and  $\tilde{Z}_j^f$  exist under the conditions of [Assumption 2.2](#). For each global  $\omega \geq 0$ , the shrinkage parameter for the  $j$ -th problem is defined as  $\omega_j := \omega / (\omega + \tilde{\sigma}_j^2)$ . Then, following the result in [Theorem A.1](#), CURE for  $\hat{\theta}_{j, \omega_j}^{\text{PAS}} := \omega_j \hat{\theta}_j^{\text{PT}} + (1 - \omega_j) \tilde{Z}_j^f$ ,

$$\text{CURE} \left( \hat{\theta}_{j, \omega}^{\text{PAS}} \right) = (2\omega_j - 1) \tilde{\sigma}_j^2 + 2(1 - \omega_j) \tilde{\gamma}_j + \left[ (1 - \omega_j) (\hat{\theta}_j^{\text{PT}} - \tilde{Z}_j^f) \right]^2,$$

is an unbiased estimator of the risk, i.e.,

$$\mathbb{E}_{\eta_j} \left[ \text{CURE} \left( \hat{\theta}_{j, \omega}^{\text{PAS}} \right) \right] = R(\hat{\theta}_{j, \omega_j}^{\text{PAS}}, \theta_j).$$

Finally, the CURE for the collection of estimators is  $\hat{\boldsymbol{\theta}}_\omega^{\text{PAS}} := (\hat{\theta}_{1, \omega}^{\text{PAS}}, \dots, \hat{\theta}_{m, \omega}^{\text{PAS}})^\top$

$$\text{CURE} \left( \hat{\boldsymbol{\theta}}_\omega^{\text{PAS}} \right) := \frac{1}{m} \sum_{j=1}^m \text{CURE} \left( \hat{\theta}_{j, \omega}^{\text{PAS}} \right),$$

which is an unbiased estimator of the compound risk  $\mathcal{R}_m(\hat{\boldsymbol{\theta}}_\omega^{\text{PAS}}, \boldsymbol{\theta})$  by linearity of the expectation.  $\square$

### B.2 Formal conditions and proof of Proposition 5.1

We aim to prove that CURE converges uniformly to the true squared-error loss  $\ell_m(\hat{\boldsymbol{\theta}}_\omega^{\text{PAS}}, \boldsymbol{\theta})$  as  $m \rightarrow \infty$ . Specifically, our goal is to establish

$$\sup_{\omega \geq 0} \left| \text{CURE}(\hat{\boldsymbol{\theta}}_\omega^{\text{PAS}}) - \ell_m(\hat{\boldsymbol{\theta}}_\omega^{\text{PAS}}, \boldsymbol{\theta}) \right| \xrightarrow[m \rightarrow \infty]{L^1} 0.$$

For this proposition, all the expectation and variance terms without subscript are conditioning on  $\boldsymbol{\eta}$ . We keep using the notations  $\theta_j = \mathbb{E}[\hat{\theta}_j^{\text{PT}}]$ ,  $\mu_j = \mathbb{E}[\tilde{Z}_j^f]$ ,  $\tilde{\sigma}_j^2 = \text{Var}[\hat{\theta}_j^{\text{PT}}]$  and  $\tilde{\gamma}_j = \text{Cov}[\hat{\theta}_j^{\text{PT}}, \tilde{Z}_j^f]$ . For this proposition, additional assumptions are placed on the data generating process (integrated over  $\mathbb{P}_\eta$ ). We first show how they translate to moment conditions on the estimators  $\hat{\theta}_j^{\text{PT}}$  and  $\tilde{Z}_j^f$ .

**Lemma B.1.** *Under the assumptions of Proposition 5.1, and specifically  $\mathbb{E}_{\mathbb{P}_\eta}[f(X_{ij})^4] < \infty$  and  $\mathbb{E}_{\mathbb{P}_\eta}[Y_{ij}^4] < \infty$ , it holds that:*

$$\begin{aligned} \sup_{j \geq 1} \mathbb{E}_{\mathbb{P}_\eta} [(\hat{\theta}_j^{\text{PT}})^4] &< \infty, & \sup_{j \geq 1} \mathbb{E}_{\mathbb{P}_\eta} [(\tilde{Z}_j^f)^4] &< \infty, \\ \mathbb{E}_{\mathbb{P}_\eta} [\theta_j^4] &< \infty, & \mathbb{E}_{\mathbb{P}_\eta} [\mu_j^4] &< \infty. \end{aligned}$$

*Proof.* By Minkowski's inequality, we have

$$\begin{aligned} \mathbb{E}_{\mathbb{P}_\eta} [(\hat{\theta}_j^{\text{PT}})^4] &= \mathbb{E}_{\mathbb{P}_\eta} [(\bar{Y}_j + \lambda_j^*(\tilde{Z}_j^f - \bar{Z}_j^f))^4] \\ &\leq \left( \mathbb{E}_{\mathbb{P}_\eta} [\bar{Y}_j^4]^{1/4} + \lambda_j^* \mathbb{E}_{\mathbb{P}_\eta} [(\tilde{Z}_j^f)^4]^{1/4} + \lambda_j^* \mathbb{E}_{\mathbb{P}_\eta} [(\bar{Z}_j^f)^4]^{1/4} \right)^4, \end{aligned}$$

so it suffices to bound the fourth moments of  $\bar{Y}_j, \tilde{Z}_j, \bar{Z}_j$ . We proceed with  $\bar{Y}_j$  first. Again, by Minkowski's inequality

$$\begin{aligned} \mathbb{E}_{\mathbb{P}_\eta} [\bar{Y}_j^4]^{1/4} &= \mathbb{E}_{\mathbb{P}_\eta} \left[ \left( \sum_{i=1}^{n_j} n_j^{-1} Y_{ij} \right)^4 \right]^{1/4} \\ &\leq \sum_{i=1}^{n_j} \mathbb{E}_{\mathbb{P}_\eta} [(n_j^{-1} Y_{ij})^4]^{1/4} \\ &= \sum_{i=1}^{n_j} n_j^{-1} \mathbb{E}_{\mathbb{P}_\eta} [Y_{ij}^4]^{1/4} \\ &= \mathbb{E}_{\mathbb{P}_\eta} [Y_{ij}^4]^{1/4} < \infty. \end{aligned}$$

The given assumption on the data generating process is used in the last line. Although the left-hand side of the inequality may depend on  $j$  (via the deterministic  $n_j$ ), the right-hand side does not depend on  $j$  (since we are integrating over  $\mathbb{P}_\eta$ ) and so we may take a supremum over all  $j$  on the left-hand side. The arguments for  $\tilde{Z}_j$  and  $\bar{Z}_j$  based on the finiteness of  $\mathbb{E}_{\mathbb{P}_\eta}[f(X_{ij})^4]$  are analogous. Next, by Jensen's inequality we have

$$\begin{aligned} \theta_j^4 &= \mathbb{E}_{\eta_j} [\hat{\theta}_j^{\text{PT}}]^4 \leq \mathbb{E}_{\eta_j} [(\hat{\theta}_j^{\text{PT}})^4] \\ \implies \mathbb{E}_{\mathbb{P}_\eta} [\theta_j^4] &\leq \mathbb{E}_{\mathbb{P}_\eta} [(\hat{\theta}_j^{\text{PT}})^4] < \infty, \end{aligned}$$

and similarly we can also obtain  $\mathbb{E}_{\mathbb{P}_\eta} [\mu_j^4] < \infty$ . □

With Lemma B.1, we will prove Proposition 5.1 via the following steps.

**Step 1: Decompose the difference.** We first decompose both CURE and the loss separately as

$$\begin{aligned}
\text{CURE}(\hat{\boldsymbol{\theta}}_{\omega}^{\text{PAS}}) &= \frac{1}{m} \sum_{j=1}^m \left( (2\omega_j - 1)\tilde{\sigma}_j^2 + \left[ (1 - \omega_j)(\hat{\theta}_j^{\text{PT}} - \tilde{Z}_j^f) \right]^2 + 2(1 - \omega_j)\tilde{\gamma}_j \right) \\
&= \frac{1}{m} \sum_{j=1}^m \underbrace{\left( (2\omega_j - 1)\tilde{\sigma}_j^2 + (1 - \omega_j)^2(\hat{\theta}_j^{\text{PT}} - \mu_j)^2 \right)}_{\mathbb{I}(\omega)} \\
&\quad + \frac{1}{m} \sum_{j=1}^m \underbrace{\left( 2(1 - \omega_j)\tilde{\gamma}_j + 2(1 - \omega_j)^2(\mu_j - \tilde{Z}_j^f)(\hat{\theta}_j^{\text{PT}} - \mu_j) + (1 - \omega_j)^2(\mu_j - \tilde{Z}_j^f)^2 \right)}_{\mathbb{III}(\omega)} \\
\ell_m(\hat{\boldsymbol{\theta}}_{\omega}^{\text{PAS}}, \boldsymbol{\theta}) &= \frac{1}{m} \sum_{j=1}^m (\omega_j \hat{\theta}_j^{\text{PT}} + (1 - \omega_j)\tilde{Z}_j^f - \theta_j)^2 \\
&= \frac{1}{m} \sum_{j=1}^m \underbrace{(\omega_j \hat{\theta}_j^{\text{PT}} + (1 - \omega_j)\mu_j - \theta_j)^2}_{\mathbb{I}^*(\omega)} \\
&\quad + \frac{1}{m} \sum_{j=1}^m \underbrace{\left( 2(1 - \omega_j)(\tilde{Z}_j^f - \mu_j)(\hat{\theta}_j^{\text{PT}} - \theta_j) + 2(1 - \omega_j)^2(\mu_j - \tilde{Z}_j^f)(\hat{\theta}_j^{\text{PT}} - \mu_j) + (1 - \omega_j)^2(\mu_j - \tilde{Z}_j^f)^2 \right)}_{\mathbb{III}^*(\omega)},
\end{aligned}$$

and we are interested in bounding

$$\sup_{\omega \geq 0} \left| \text{CURE}(\hat{\boldsymbol{\theta}}_{\omega}^{\text{PAS}}) - \ell_m(\hat{\boldsymbol{\theta}}_{\omega}^{\text{PAS}}, \boldsymbol{\theta}) \right| \leq \sup_{\omega \geq 0} |\mathbb{I}(\omega) - \mathbb{I}^*(\omega)| + \sup_{\omega \geq 0} |\mathbb{III}(\omega) - \mathbb{III}^*(\omega)|. \quad (21)$$

**Step 2: Bounding the first difference  $\Delta_1(\omega) := \mathbb{I}(\omega) - \mathbb{I}^*(\omega)$ .** The proof in this step is directly adapted from **Theorem 5.1** in [Xie et al. \[2012\]](#) and generalizes to non-Gaussian data. With some algebraic manipulation, we can further decompose

$$\begin{aligned}
\Delta_1(\omega) &= \frac{1}{m} \sum_{j=1}^m \left( (2\omega_j - 1)\tilde{\sigma}_j^2 + (1 - \omega_j)^2(\hat{\theta}_j^{\text{PT}} - \mu_j)^2 \right) \\
&\quad - \frac{1}{m} \sum_{j=1}^m (\omega_j \hat{\theta}_j^{\text{PT}} + (1 - \omega_j)\mu_j - \theta_j)^2 \\
&= \text{CURE}(\hat{\boldsymbol{\theta}}_{\omega}^0) - \ell_m(\hat{\boldsymbol{\theta}}_{\omega}^0, \boldsymbol{\theta}) - \frac{2}{m} \sum_{j=1}^m \mu_j(1 - \omega_j)(\hat{\theta}_j^{\text{PT}} - \theta_j)
\end{aligned}$$

$$\text{where } \text{CURE}(\hat{\boldsymbol{\theta}}_{\omega}^0) = \frac{1}{m} \sum_{j=1}^m \left( (2\omega_j - 1)\tilde{\sigma}_j^2 + (1 - \omega_j)^2(\hat{\theta}_j^{\text{PT}})^2 \right), \quad \ell_m(\hat{\boldsymbol{\theta}}_{\omega}^0, \boldsymbol{\theta}) = \frac{1}{m} \sum_{j=1}^m (\omega_j \hat{\theta}_j^{\text{PT}} - \theta_j)^2,$$

corresponds to CURE and the loss of the “shrink-towards-zero” estimator  $\hat{\theta}_{j,\omega}^0 := \omega_j \hat{\theta}_j^{\text{PT}}$ . We thus have

$$\sup_{\omega \geq 0} |\Delta_1(\omega)| \leq \sup_{\omega \geq 0} \left| \text{CURE}(\hat{\boldsymbol{\theta}}_{\omega}^0) - \ell_m(\hat{\boldsymbol{\theta}}_{\omega}^0, \boldsymbol{\theta}) \right| + \frac{2}{m} \sup_{\omega \geq 0} \left| \sum_{j=1}^m \mu_j(1 - \omega_j)(\hat{\theta}_j^{\text{PT}} - \theta_j) \right|. \quad (22)$$

Now, rearrangements of terms gives that

$$\begin{aligned}
\sup_{\omega \geq 0} \left| \text{CURE}(\hat{\boldsymbol{\theta}}_{\omega}^0) - \ell_m(\hat{\boldsymbol{\theta}}_{\omega}^0, \boldsymbol{\theta}) \right| &= \sup_{\omega \geq 0} \left| \frac{1}{m} \sum_{j=1}^m \left( (\hat{\theta}_j^{\text{PT}})^2 - \tilde{\sigma}_j^2 - \theta_j^2 - 2\omega_j \left( (\hat{\theta}_j^{\text{PT}})^2 - \hat{\theta}_j^{\text{PT}}\theta_j - \tilde{\sigma}_j^2 \right) \right) \right| \\
&\leq \underbrace{\left| \frac{1}{m} \sum_{j=1}^m (\hat{\theta}_j^{\text{PT}})^2 - \tilde{\sigma}_j^2 - \theta_j^2 \right|}_{(*)} + \sup_{\omega \geq 0} \underbrace{\left| \frac{1}{m} \sum_{j=1}^m 2\omega_j \left( (\hat{\theta}_j^{\text{PT}})^2 - \hat{\theta}_j^{\text{PT}}\theta_j - \tilde{\sigma}_j^2 \right) \right|}_{(**)}.
\end{aligned}$$

For the first term (\*),

$$\mathbb{E}_{\mathbb{P}_\eta} \left[ \mathbb{E}_\eta \left[ \left( \frac{1}{m} \sum_{j=1}^m (\hat{\theta}_j^{\text{PT}})^2 - \tilde{\sigma}_j^2 - \theta_j^2 \right)^2 \right] \right] = \frac{1}{m^2} \sum_{j=1}^m \mathbb{E}_{\mathbb{P}_\eta} \left[ \text{Var}_{\eta_j} \left[ (\hat{\theta}_j^{\text{PT}})^2 \right] \right] \leq \frac{1}{m} \sup_j \text{Var}_{\mathbb{P}_\eta} \left[ (\hat{\theta}_j^{\text{PT}})^2 \right].$$

Thus by Jensen's inequality and iterated expectation:

$$\mathbb{E}_{\mathbb{P}_\eta} \left[ \left| \frac{1}{m} \sum_{j=1}^m (\hat{\theta}_j^{\text{PT}})^2 - \tilde{\sigma}_j^2 - \theta_j^2 \right| \right] \leq \left( \frac{1}{m} \sup_j \text{Var}_{\mathbb{P}_\eta} \left[ (\hat{\theta}_j^{\text{PT}})^2 \right] \right)^{1/2}. \quad (23)$$

For the second term (\*\*), we start by arguing conditionally on  $\boldsymbol{\eta}$ , which implies in particular that we may treat all the  $\tilde{\sigma}_j^2$  as fixed. It is thus without loss of generality to assume that  $\tilde{\sigma}_1^2 \leq \dots \leq \tilde{\sigma}_m^2$  (by first sorting problems according to the value of  $\tilde{\sigma}_j^2$ ). Then, since  $\omega_j$  is monotonic function of  $\tilde{\sigma}_j^2$  for any fixed  $\omega \geq 0$ , we have  $1 \geq \omega_1 \geq \dots \geq \omega_m \geq 0$ . The following inequality follows:

$$\sup_{\omega \geq 0} \left| \frac{1}{m} \sum_{j=1}^m 2\omega_j \left( (\hat{\theta}_j^{\text{PT}})^2 - \hat{\theta}_j^{\text{PT}} \theta_j - \tilde{\sigma}_j^2 \right) \right| \leq \max_{1 \geq c_1 \geq \dots \geq c_m \geq 0} \left| \frac{2}{m} \sum_{j=1}^m c_j \left( (\hat{\theta}_j^{\text{PT}})^2 - \hat{\theta}_j^{\text{PT}} \theta_j - \tilde{\sigma}_j^2 \right) \right|. \quad (24)$$

The following lemma would help us for handling the RHS of (24) (the same structural form of it will appear repeatedly in subsequent parts of the proof).

**Lemma B.2.** *Let  $A_1, \dots, A_n$  be real numbers. Then*

$$\max_{1 \geq c_1 \geq \dots \geq c_n \geq 0} \left| \sum_{i=1}^n c_i A_i \right| = \max_{1 \leq k \leq n} \left| \sum_{i=1}^k A_i \right|.$$

*Proof.* Define  $S_k = \sum_{i=1}^k A_i$  for  $k = 1, \dots, n$ , and let  $c_1, \dots, c_n$  be real numbers satisfying  $1 \geq c_1 \geq \dots \geq c_n \geq 0$ . Set  $c_{n+1} = 0$ . Then we can rewrite

$$\sum_{i=1}^n c_i A_i = \sum_{k=1}^n (c_k - c_{k+1}) \left( \sum_{i=1}^k A_i \right) = \sum_{k=1}^n (c_k - c_{k+1}) S_k.$$

Since  $c_k \geq c_{k+1}$ , each  $\alpha_k := c_k - c_{k+1}$  is nonnegative, and

$$\sum_{k=1}^n \alpha_k = c_1 - c_{n+1} \leq 1.$$

Hence,

$$\left| \sum_{i=1}^n c_i A_i \right| = \left| \sum_{k=1}^n \alpha_k S_k \right| \leq \sum_{k=1}^n \alpha_k |S_k| \leq \left( \max_{1 \leq k \leq n} |S_k| \right) \left( \sum_{k=1}^n \alpha_k \right) \leq \max_{1 \leq k \leq n} |S_k|.$$

This shows

$$\max_{1 \geq c_1 \geq \dots \geq c_n \geq 0} \left| \sum_{i=1}^n c_i A_i \right| \leq \max_{1 \leq k \leq n} \left| \sum_{i=1}^k A_i \right|.$$

To see that this upper bound can be attained, consider for each  $k$  the choice

$$c_1 = c_2 = \dots = c_k = 1, \quad c_{k+1} = c_{k+2} = \dots = c_n = 0.$$

Since  $1 \geq c_1 \geq \dots \geq c_n \geq 0$ , we have that

$$\left| \sum_{i=1}^n c_i A_i \right| = \left| \sum_{i=1}^k A_i \right| = |S_k|.$$

Taking the maximum over all such  $k \in \{1, \dots, n\}$  matches  $\max_{1 \leq k \leq n} |S_k|$ . Thus,

$$\max_{1 \geq c_1 \geq \dots \geq c_n \geq 0} \left| \sum_{i=1}^n c_i A_i \right| = \max_{1 \leq k \leq n} \left| \sum_{i=1}^k A_i \right|,$$

as claimed.  $\square$

With Lemma B.2 in hand, we have

$$\max_{1 \geq c_1 \geq \dots \geq c_m \geq 0} \left| \frac{2}{m} \sum_{j=1}^m c_j \left( (\hat{\theta}_j^{\text{PT}})^2 - \hat{\theta}_j^{\text{PT}} \theta_j - \tilde{\sigma}_j^2 \right) \right| = \max_{1 \leq k \leq m} \left| \frac{2}{m} \sum_{j=1}^k \left( (\hat{\theta}_j^{\text{PT}})^2 - \hat{\theta}_j^{\text{PT}} \theta_j - \tilde{\sigma}_j^2 \right) \right|.$$

Let  $M_k := \sum_{j=1}^k \left( (\hat{\theta}_j^{\text{PT}})^2 - \hat{\theta}_j^{\text{PT}} \theta_j - \tilde{\sigma}_j^2 \right)$ , it is easy to see that  $\{M_k\}_{k=1}^m$  forms a martingale conditional on  $\boldsymbol{\eta}$ . Therefore, by a standard  $L^2$  maximal inequality (ref. Theorem 4.4.6 in Durrett [2019]), we have

$$\mathbb{E}_{\boldsymbol{\eta}} \left[ \max_{1 \leq k \leq m} M_k^2 \right] \leq 4 \mathbb{E}_{\boldsymbol{\eta}} [M_m^2] = 4 \sum_{j=1}^m \text{Var}_{\eta_j} \left[ (\hat{\theta}_j^{\text{PT}})^2 - \hat{\theta}_j^{\text{PT}} \theta_j \right], \quad (25)$$

which then implies

$$\begin{aligned} \mathbb{E}_{\mathbb{P}_{\boldsymbol{\eta}}} \left[ \left( \sup_{\omega \geq 0} \left| \frac{1}{m} \sum_{j=1}^m 2\omega_j \left( (\hat{\theta}_j^{\text{PT}})^2 - \hat{\theta}_j^{\text{PT}} \theta_j - \tilde{\sigma}_j^2 \right) \right| \right)^2 \right] &\leq \frac{4}{m^2} \mathbb{E}_{\mathbb{P}_{\boldsymbol{\eta}}} \left[ \max_{1 \leq k \leq m} M_k^2 \right] \\ &= \frac{16}{m^2} \sum_{j=1}^m \mathbb{E}_{\mathbb{P}_{\boldsymbol{\eta}}} \left[ \text{Var}_{\eta_j} \left[ (\hat{\theta}_j^{\text{PT}})^2 - \hat{\theta}_j^{\text{PT}} \theta_j \right] \right] \\ &\leq \frac{16}{m} \sup_j \text{Var}_{\mathbb{P}_{\boldsymbol{\eta}}} \left[ (\hat{\theta}_j^{\text{PT}})^2 - \hat{\theta}_j^{\text{PT}} \theta_j \right] \\ \implies \mathbb{E}_{\mathbb{P}_{\boldsymbol{\eta}}} \left[ \sup_{\omega \geq 0} \left| \frac{1}{m} \sum_{j=1}^m 2\omega_j \left( (\hat{\theta}_j^{\text{PT}})^2 - \hat{\theta}_j^{\text{PT}} \theta_j - \tilde{\sigma}_j^2 \right) \right| \right] &\leq \left( \frac{16}{m} \sup_j \text{Var}_{\mathbb{P}_{\boldsymbol{\eta}}} \left[ (\hat{\theta}_j^{\text{PT}})^2 - \hat{\theta}_j^{\text{PT}} \theta_j \right] \right)^{1/2}. \quad (26) \end{aligned}$$

Next, we bound the last expression in (22):  $\frac{2}{m} \sup_{\omega \geq 0} \left| \sum_{j=1}^m (1 - \omega_j) \mu_j (\hat{\theta}_j^{\text{PT}} - \theta_j) \right|$ . Note that  $(1 - \omega_j)$  is also monotonic in  $\tilde{\sigma}_j^2$ , and if we define  $M'_k := \sum_{j=1}^k \mu_j (\hat{\theta}_j^{\text{PT}} - \theta_j)$ , then  $\{M'_k\}_{k=1}^m$  forms another martingale conditioning on  $\boldsymbol{\eta}$ . Therefore, following the same argument as (24)–(25) gives

$$\begin{aligned} \frac{4}{m^2} \mathbb{E}_{\mathbb{P}_{\boldsymbol{\eta}}} \left[ \sup_{\omega \geq 0} \left| \sum_{j=1}^m (1 - \omega_j) \mu_j (\hat{\theta}_j^{\text{PT}} - \theta_j) \right|^2 \right] &\leq \frac{4}{m^2} \mathbb{E}_{\mathbb{P}_{\boldsymbol{\eta}}} \left[ \max_{1 \leq k \leq m} M_k'^2 \right] \\ &\leq \frac{16}{m^2} \mathbb{E}_{\mathbb{P}_{\boldsymbol{\eta}}} [M_m'^2] = \frac{16}{m} \sup_j \mathbb{E}_{\mathbb{P}_{\boldsymbol{\eta}}} \left[ \text{Var}_{\eta_j} \left[ \hat{\theta}_j^{\text{PT}} \right] \mu_j^2 \right] \\ \implies \mathbb{E}_{\mathbb{P}_{\boldsymbol{\eta}}} \left[ \frac{2}{m} \sup_{\omega \geq 0} \left| \sum_{j=1}^m (1 - \omega_j) \mu_j (\hat{\theta}_j^{\text{PT}} - \theta_j) \right| \right] &\leq \left( \frac{16}{m} \sup_j \mathbb{E}_{\mathbb{P}_{\boldsymbol{\eta}}} \left[ \text{Var}_{\eta_j} \left[ \hat{\theta}_j^{\text{PT}} \right] \mu_j^2 \right] \right)^{1/2}. \quad (27) \end{aligned}$$

The upper bounds derived in (23), (26) and (27) establish control on

$$\mathbb{E}_{\mathbb{P}_{\boldsymbol{\eta}}} \left[ \sup_{\omega \geq 0} |\Delta_1(\omega)| \right] \leq \frac{4}{\sqrt{m}} \left( \sup_j \text{Var}_{\mathbb{P}_{\boldsymbol{\eta}}} \left[ (\hat{\theta}_j^{\text{PT}})^2 \right]^{1/2} + \sup_j \text{Var}_{\mathbb{P}_{\boldsymbol{\eta}}} \left[ (\hat{\theta}_j^{\text{PT}})^2 - \hat{\theta}_j^{\text{PT}} \theta_j \right] + \sup_j \mathbb{E}_{\mathbb{P}_{\boldsymbol{\eta}}} \left[ \text{Var}_{\eta_j} \left[ \hat{\theta}_j^{\text{PT}} \right] \mu_j^2 \right] \right),$$

since each term on the right-hand side can be controlled by the fourth-moment conditions established in Lemma B.1, we know that  $\Delta_1(\omega)$  converges uniformly to zero.

**Step 3: Bounding the second difference**  $\Delta_2(\omega) := \text{III}(\omega) - \text{III}^*(\omega)$ . We next cancel out identical terms in the second difference in (21) and get

$$\Delta_2(\omega) = \frac{2}{m} \sum_{j=1}^m (1 - \omega_j) [\tilde{\gamma}_j - (\tilde{Z}_j^f - \mu_j) (\hat{\theta}_j^{\text{PT}} - \theta_j)]. \quad (28)$$

By the same proof logic that has been applied twice above, we now have a function  $(1 - \omega_j)$  monotonic in  $\tilde{\sigma}_j^2$ , and a martingale  $Q_k := \sum_{j=1}^k [\tilde{\gamma}_j - (\tilde{Z}_j^f - \mu_j) (\hat{\theta}_j^{\text{PT}} - \theta_j)]$  for  $k = 1, \dots, m$  (recall that  $\tilde{\gamma}_j =$

$\text{Cov}_{\eta_j}[\hat{\theta}_j^{\text{PT}}, \tilde{Z}_j^f]$ ). The steps from (24)–(25) follows, and we have

$$\frac{4}{m^2} \mathbb{E}_{\mathbb{P}_\eta} \left[ \left( \sup_{\omega \geq 0} \left| \sum_{j=1}^m (1 - \omega_j) [\tilde{\gamma}_j - (\tilde{Z}_j^f - \mu_j)(\hat{\theta}_j^{\text{PT}} - \theta_j)] \right| \right)^2 \right] \leq \frac{16}{m} \sup_j \mathbb{E}_{\mathbb{P}_\eta} \left[ \text{Var}_{\eta_j} \left[ (\tilde{Z}_j^f - \mu_j)(\hat{\theta}_j^{\text{PT}} - \theta_j) \right] \right],$$

and so,

$$\mathbb{E}_{\mathbb{P}_\eta} \left[ \frac{2}{m} \sup_{\omega \geq 0} \left| \sum_{j=1}^m (1 - \omega_j) [\tilde{\gamma}_j - (\tilde{Z}_j^f - \mu_j)(\hat{\theta}_j^{\text{PT}} - \theta_j)] \right| \right] \leq \left( \frac{16}{m} \sup_j \mathbb{E}_{\mathbb{P}_\eta} \left[ \text{Var}_{\eta_j} \left[ (\tilde{Z}_j^f - \mu_j)(\hat{\theta}_j^{\text{PT}} - \theta_j) \right] \right] \right)^{1/2}.$$

Again, the (fourth-)moment conditions from Lemma B.1 suffice to ensure that

$$\sup_j \mathbb{E}_{\mathbb{P}_\eta} \left[ \text{Var}_{\eta_j} \left[ (\tilde{Z}_j^f - \mu_j)(\hat{\theta}_j^{\text{PT}} - \theta_j) \right] \right] < \infty,$$

and to establish control of

$$\mathbb{E}_{\mathbb{P}_\eta} \left[ \sup_{\omega \geq 0} |\Delta_2(\omega)| \right].$$

**Step 4: Concluding the argument.** Finally, based on Steps 1–3, we have that

$$\mathbb{E}_{\mathbb{P}_\eta} \left[ \sup_{\omega \geq 0} \left| \text{CURE}(\hat{\theta}_\omega^{\text{PAS}}) - \ell_m(\hat{\theta}_\omega^{\text{PAS}}, \theta) \right| \right] \leq \mathbb{E}_{\mathbb{P}_\eta} \left[ \sup_{\omega \geq 0} |\Delta_1(\omega)| \right] + \mathbb{E}_{\mathbb{P}_\eta} \left[ \sup_{\omega \geq 0} |\Delta_2(\omega)| \right],$$

and both terms on the right hand side converge to zero by our preceding bounds and the moment assumptions in the statement of the theorem.  $\square$

### B.3 Proof of Theorem 5.2

We apply a standard argument used to prove consistency of M-estimators.

Let  $\omega_*$  be the oracle choice of  $\omega \geq 0$  that minimizes the Bayes risk  $\mathcal{B}_m^{\mathbb{P}_\eta}(\hat{\theta}_{\omega_*}^{\text{PAS}})$ .<sup>10</sup> Notice that by definition of  $\hat{\omega}$  as the minimizer of CURE,

$$\text{CURE}(\hat{\theta}_{\hat{\omega}}^{\text{PAS}}) \leq \text{CURE}(\hat{\theta}_{\omega_*}^{\text{PAS}}).$$

Then:

$$\ell_m(\hat{\theta}_{\hat{\omega}}^{\text{PAS}}, \theta) - \ell_m(\hat{\theta}_{\omega_*}^{\text{PAS}}, \theta) \leq 2 \sup_{\omega \geq 0} \left| \text{CURE}(\hat{\theta}_\omega^{\text{PAS}}) - \ell_m(\hat{\theta}_\omega^{\text{PAS}}, \theta) \right|.$$

Taking expectations,

$$\mathcal{B}_m^{\mathbb{P}_\eta}(\hat{\theta}_{\hat{\omega}}^{\text{PAS}}) - \mathcal{B}_m^{\mathbb{P}_\eta}(\hat{\theta}_{\omega_*}^{\text{PAS}}) \leq 2 \mathbb{E}_{\mathbb{P}_\eta} \left[ \sup_{\omega \geq 0} \left| \text{CURE}(\hat{\theta}_\omega^{\text{PAS}}) - \ell_m(\hat{\theta}_\omega^{\text{PAS}}, \theta) \right| \right].$$

Noting that the right hand side converges to 0 as  $m \rightarrow \infty$ , and recalling the definition of  $\omega_*$ , we prove the desired result

$$\mathcal{B}_m^{\mathbb{P}_\eta}(\hat{\theta}_{\hat{\omega}}^{\text{PAS}}) \leq \inf_{\omega \geq 0} \mathcal{B}_m^{\mathbb{P}_\eta}(\hat{\theta}_\omega^{\text{PAS}}) + o(1).$$

$\square$

---

<sup>10</sup>To streamline the proof, we assume that the infimum is attained by a value  $\omega_*$ . If the infimum is not attained, the proof still goes through using approximate minimizers.



## B.4 Proof of Proposition 5.3

We start with the result in Theorem 5.2

$$\mathcal{B}_m^{\mathbb{P}_\eta}(\hat{\boldsymbol{\theta}}_{\tilde{\omega}}^{\text{PAS}}, \boldsymbol{\theta}) \leq \inf_{\omega \geq 0} \mathcal{B}_m^{\mathbb{P}_\eta}(\hat{\boldsymbol{\theta}}_{\omega}^{\text{PAS}}, \boldsymbol{\theta}) + o(1).$$

Now, since we are integrating over  $\eta \sim \mathbb{P}_\eta$  for all problems

$$\begin{aligned} \mathcal{B}_m^{\mathbb{P}_\eta}(\hat{\boldsymbol{\theta}}_{\omega}^{\text{PAS}}, \boldsymbol{\theta}) &= \frac{1}{m} \sum_{j=1}^m \mathbb{E}_{\mathbb{P}_\eta} \left[ (\hat{\theta}_{j,\omega}^{\text{PAS}} - \theta_j)^2 \right] \\ &= \mathbb{E}_{\mathbb{P}_\eta} \left[ (\hat{\theta}_{j,\omega}^{\text{PAS}} - \theta_j)^2 \right], \end{aligned}$$

by definition  $\hat{\theta}_{j,\omega}^{\text{PAS}} = \omega_j \hat{\theta}_j^{\text{PT}} + (1 - \omega_j) \tilde{Z}_j^f$ , where  $\omega_j = \omega/(\omega + \tilde{\sigma}^2)$ . Therefore

$$\begin{aligned} \mathbb{E}_{\mathbb{P}_\eta} \left[ (\hat{\theta}_{j,\omega}^{\text{PAS}} - \theta_j)^2 \right] &= \mathbb{E}_{\mathbb{P}_\eta} \left[ (\omega_j (\hat{\theta}_j^{\text{PT}} - \theta_j) + (1 - \omega_j) (\tilde{Z}_j^f - \theta_j))^2 \right] \\ &= \frac{\omega^2}{(\omega + \tilde{\sigma}^2)^2} \mathbb{E}_{\mathbb{P}_\eta} \left[ (\hat{\theta}_j^{\text{PT}} - \theta_j)^2 \right] + \frac{\tilde{\sigma}^4}{(\omega + \tilde{\sigma}^2)^2} \mathbb{E}_{\mathbb{P}_\eta} \left[ (\tilde{Z}_j^f - \theta_j)^2 \right] \\ &\quad + 2 \frac{\tilde{\sigma}^2 \omega}{(\omega + \tilde{\sigma}^2)^2} \mathbb{E}_{\mathbb{P}_\eta} \left[ (\hat{\theta}_j^{\text{PT}} - \theta_j) (\tilde{Z}_j^f - \theta_j) \right]. \end{aligned}$$

By our assumption, second moment terms like  $\tilde{\sigma}^2$  and  $\tilde{\gamma}$  are now fixed, so we have (by iterated expectation)

$$\mathbb{E}_{\mathbb{P}_\eta} \left[ (\hat{\theta}_j^{\text{PT}} - \theta_j)^2 \right] = \tilde{\sigma}^2.$$

Noting that  $\tilde{\gamma}_j = 0$  since  $N_j = \infty$ , we have

$$\mathbb{E}_{\mathbb{P}_\eta} \left[ (\hat{\theta}_{j,\omega}^{\text{PAS}} - \theta_j)^2 \right] = \frac{\omega^2 \tilde{\sigma}^2}{(\omega + \tilde{\sigma}^2)^2} + \frac{\tilde{\sigma}^4}{(\omega + \tilde{\sigma}^2)^2} \mathbb{E}_{\mathbb{P}_\eta} \left[ (\tilde{Z}_j^f - \theta_j)^2 \right].$$

Plugging in  $\omega = \mathbb{E}_{\mathbb{P}_\eta} \left[ (\tilde{Z}_j^f - \theta_j)^2 \right]$  gives

$$\frac{\omega^2 \tilde{\sigma}^2}{(\omega + \tilde{\sigma}^2)^2} + \frac{\tilde{\sigma}^4}{(\omega + \tilde{\sigma}^2)^2} \mathbb{E}_{\mathbb{P}_\eta} \left[ (\tilde{Z}_j^f - \theta_j)^2 \right] = \frac{\tilde{\sigma}^2 \mathbb{E}_{\mathbb{P}_\eta} \left[ (\tilde{Z}_j^f - \theta_j)^2 \right]}{\tilde{\sigma}^2 + \mathbb{E}_{\mathbb{P}_\eta} \left[ (\tilde{Z}_j^f - \theta_j)^2 \right]}.$$

We finally have

$$\mathcal{B}_m^{\mathbb{P}_\eta}(\hat{\boldsymbol{\theta}}^{\text{PAS}}) \leq \frac{\tilde{\sigma}^2 \mathbb{E}_{\mathbb{P}_\eta} \left[ (\tilde{Z}_j^f - \theta_j)^2 \right]}{\tilde{\sigma}^2 + \mathbb{E}_{\mathbb{P}_\eta} \left[ (\tilde{Z}_j^f - \theta_j)^2 \right]} + o(1).$$

□

## C Other Baseline Shrinkage Estimators

### C.1 “Shrink-classical” (Shrinkage) Baseline

The “shrink-classical” estimator applies shrinkage directly to the classical estimator  $\bar{Y}_j$ , using the prediction mean  $\tilde{Z}_j^f$  as a shrinkage target *without* first applying power-tuned PPI. We include this baseline to isolate the benefits of power tuning from the PAS estimator as an ablation study.

**Formulation.** The “shrink-classical” estimator for problem  $j$  takes the form:

$$\begin{aligned} \hat{\theta}_{j,\omega}^{\text{Shrink}} &:= \omega_j \bar{Y}_j + (1 - \omega_j) \tilde{Z}_j^f, \\ \text{where } \omega_j &:= \omega/(\omega + \tilde{\sigma}_j^2), \quad \tilde{\sigma}_j^2 := \text{Var}_{\eta_j}[\bar{Y}_j] = \sigma_j^2/n_j. \end{aligned}$$

Here  $\omega \geq 0$  is a global shrinkage parameter analogous to Section 4.2. The key difference from PAS is that we shrink the classical estimator  $\bar{Y}_j$  (which is independent of  $\tilde{Z}_j^f$ ) rather than the power-tuned estimator  $\hat{\theta}_j^{\text{PT}}$  (which is correlated with  $\tilde{Z}_j^f$ ).

**Optimizing  $\omega$  via CURE.** Since  $\bar{Y}_j$  and  $\tilde{Z}_j^f$  are independent, Theorem 4.1 simplifies. Let  $\tilde{\gamma}_j = \text{Cov}[\bar{Y}_j, \tilde{Z}_j^f] = 0$  and  $\tilde{\sigma}_j^2 = \sigma_j^2/n_j$ . CURE simplifies as:

$$\text{CURE}(\hat{\theta}_{j,\omega}^{\text{Shrink}}) = (2\omega_j - 1)\tilde{\sigma}_j^2 + \left[ (1 - \omega_j)(\bar{Y}_j - \tilde{Z}_j^f) \right]^2.$$

This follows from Theorem 4.1 by setting  $\tilde{\gamma}_j = 0$ . The global shrinkage parameter  $\omega$  is selected by minimizing CURE across all  $m$  problems.

$$\begin{aligned} \hat{\theta}_j^{\text{Shrink}} &:= \hat{\omega}_j \bar{Y}_j + (1 - \hat{\omega}_j) \tilde{Z}_j^f, \quad \hat{\omega}_j = \hat{\omega} / (\hat{\omega} + \tilde{\sigma}_j^2), \\ \text{where } \hat{\omega} &\in \arg \min_{\omega \geq 0} \frac{1}{m} \sum_{j=1}^m \text{CURE}(\hat{\theta}_{j,\omega}^{\text{Shrink}}). \end{aligned} \quad (29)$$

The optimal  $\hat{\omega}$  does not admit a closed-form expression, but we can compute it numerically by grid search. Below we provide the pseudo-code for implementing the “shrink-classical” estimator.

---

**Algorithm 2** “Shrink-classical” Estimator

---

**Require:**  $\{(X_{ij}, Y_{ij})_{i=1}^{n_j}\}, \{\tilde{X}_{ij}\}_{i=1}^{N_j}$  for  $j \in [m]$ , variance parameters  $\{\sigma_j^2\}_{j=1}^m$ , predictive model  $f$

- 1: **for**  $j = 1$  to  $m$  **do**
- 2:  $\bar{Y}_j, \tilde{Z}_j^f = \text{get\_means}((X_{ij}, Y_{ij})_{i=1}^{n_j}, (\tilde{X}_{ij})_{i=1}^{N_j}, f)$
- 3:  $\tilde{\sigma}_j^2 \leftarrow \sigma_j^2/n_j$   $\triangleright$  variance of  $\bar{Y}_j$
- 4: **end for**
- 5:  $\hat{\omega} = \text{get\_shrink\_param}(\{\bar{Y}_j\}_{j=1}^m, \{\tilde{Z}_j^f\}_{j=1}^m, \{\tilde{\sigma}_j^2\}_{j=1}^m) \triangleright$  use Eq. (29)
- 6: **for**  $j = 1$  to  $m$  **do**
- 7:  $\hat{\omega}_j = \hat{\omega} / (\hat{\omega} + \tilde{\sigma}_j^2)$
- 8:  $\hat{\theta}_j^{\text{Shrink}} = \hat{\omega}_j \bar{Y}_j + (1 - \hat{\omega}_j) \tilde{Z}_j^f$
- 9: **end for**
- 10: **return**  $\{\hat{\theta}_j^{\text{Shrink}}\}_{j=1}^m$

---

## C.2 “Shrink-average” Baseline

The “shrink-average” estimator represents an alternative, perhaps more classical, shrinkage approach that attempts to further improve upon the unbiased PT estimators. While PAS reuses the prediction means on unlabeled data as shrinkage targets, here we consider shrinking the PT estimators across all problems to a shared location, namely their group mean

$$\bar{\theta}^{\text{PT}} := \frac{1}{m} \sum_{j=1}^m \hat{\theta}_j^{\text{PT}}.$$

**Formulation.** The “shrink-average” estimator for problem  $j$  takes the form:

$$\begin{aligned} \hat{\theta}_{j,\omega}^{\text{Avg}} &:= \omega_j \hat{\theta}_j^{\text{PT}} + (1 - \omega_j) \bar{\theta}^{\text{PT}}, \\ \text{where } \omega_j &:= \omega / (\omega + \tilde{\sigma}_j^2), \quad \tilde{\sigma}_j^2 := \text{Var}_{\eta_j}[\hat{\theta}_j^{\text{PT}}]. \end{aligned}$$

**Optimizing  $\omega$  via SURE.** Xie et al. [2012] proposed the following unbiased risk estimate to optimize  $\omega$  for this estimator. Note that even though the group mean is also correlated with each PT estimator, we still denote the following SURE instead of CURE following the nomenclature in Xie et al. [2012].

$$\begin{aligned} \hat{\omega} &\in \arg \min_{\omega \geq 0} \frac{1}{m} \sum_{j=1}^m \text{SURE}(\hat{\theta}_{j,\omega}^{\text{Shrink}}) \\ \text{SURE}(\hat{\theta}_{j,\omega}^{\text{Shrink}}) &:= \left[ (1 - \omega_j)(\hat{\theta}_j^{\text{PT}} - \bar{\theta}^{\text{PT}}) \right]^2 + (1 - \omega_j)(\omega + (2/m - 1)\tilde{\sigma}_j^2). \end{aligned} \quad (30)$$

---

**Algorithm 3** “Shrink-average” Estimator
 

---

**Require:**  $(X_{ij}, Y_{ij})_{i=1}^{n_j}$ ,  $(\tilde{X}_{ij})_{i=1}^{N_j}$ ,  $\rho_j, \tau_j, \sigma_j$  for  $j \in [m]$ , predictive model  $f$

- 1: **for**  $j = 1$  to  $m$  **do**
- 2:    $\triangleright$  Step 1: Apply predictor (Eq. (1))
- 3:    $\bar{Y}_j, \bar{Z}_j^f, \tilde{Z}_j^f = \text{get\_means}((X_{ij}, Y_{ij})_{i=1}^{n_j}, (\tilde{X}_{ij})_{i=1}^{N_j}, f)$
- 4:    $\triangleright$  Step 2: Power tuning (Eq. (13))
- 5:    $\lambda_j^* = \text{get\_pt\_param}(\rho_j, \tau_j, n_j, N_j)$
- 6:    $\hat{\theta}_j^{\text{PT}} = \bar{Y}_j + \lambda_j^*(\tilde{Z}_j^f - \bar{Z}_j^f)$
- 7:    $\tilde{\sigma}_j^2 = \text{get\_pt\_var}(\hat{\theta}_j^{\text{PT}}) \triangleright$  (Eq. (14))
- 8: **end for**
- 9:  $\bar{\theta}^{\text{PT}} = m^{-1} \sum_{j=1}^m \hat{\theta}_j^{\text{PT}}$
- 10:  $\triangleright$  Step 3: Adaptive shrinkage towards group mean (Eq. (30))
- 11:  $\hat{\omega} = \text{get\_shrink\_param}(\{\hat{\theta}_j^{\text{PT}}\}_{j=1}^m, \bar{\theta}^{\text{PT}}, \{\tilde{\sigma}_j^2\}_{j=1}^m)$
- 12: **for**  $j = 1$  to  $m$  **do**
- 13:    $\hat{\omega}_j = \hat{\omega} / (\hat{\omega} + \tilde{\sigma}_j^2)$
- 14:    $\hat{\theta}_j^{\text{Avg}} = \hat{\omega}_j \hat{\theta}_j^{\text{PT}} + (1 - \hat{\omega}_j) \bar{\theta}^{\text{PT}}$
- 15: **end for**
- 16: **return**  $\{\hat{\theta}_j^{\text{Avg}}\}_{j=1}^m$

---

## D Experiment Details

### D.1 Sample-based Estimators for $\sigma_j^2, \tau_j^2, \gamma_j$

In Assumption 2.1, we assumed that the second-moment parameters  $\sigma_j^2, \tau_j^2, \gamma_j$  at the sampling level are known in order to motivate our method and streamline theoretical results. In practice, when the true data generating process is unknown or when we only have access to a black-box predictor, we plug in the following sample-based (unbiased) estimators for the parameters:

$$\hat{\sigma}_j^2 := \frac{1}{n_j - 1} \sum_{i=1}^{n_j} (Y_{ij} - \bar{Y}_j)^2, \quad \hat{\tau}_j^2 := \frac{1}{n_j + N_j - 1} \left( \sum_{i=1}^{n_j} (f(X_{ij}) - \hat{Z}_j)^2 + \sum_{i=1}^{N_j} (f(\tilde{X}_{ij}) - \hat{Z}_j)^2 \right),$$

$$\hat{\gamma}_j := \frac{1}{n_j - 1} \sum_{i=1}^{n_j} (Y_{ij} - \bar{Y}_j)(f(X_{ij}) - \bar{Z}_j^{N+n}), \quad \text{where} \quad \bar{Z}_j^{N+n} := \frac{1}{n_j + N_j} \left( \sum_{i=1}^{n_j} f(X_{ij}) + \sum_{i=1}^{N_j} f(\tilde{X}_{ij}) \right).$$

These sample-based estimators are used in our numerical experiments involving real-world datasets.

### D.2 Synthetic Model

**Motivation.** In Example 2.3, we described the following data generation process (copied from Eq. (8))

$$\eta_j \sim \mathcal{U}[-1, 1], \quad j = 1, \dots, m,$$

$$X_{ij} \sim \mathcal{N}(\eta_j, \psi^2), \quad Y_{ij} | X_{ij} \sim \mathcal{N}(2\eta_j X_{ij} - \eta_j^2, c), \quad i = 1, \dots, n_j,$$

and the same for  $(\tilde{X}_{ij}, \tilde{Y}_{ij})$ .  $\psi$  and  $c$  are two hyperparameters that we chose to be 0.1 and 0.05, respectively. The (marginal) mean and variance of  $Y_{ij}$  are

$$\theta_j := \mathbb{E}_{\eta_j}[Y_{ij}] = \eta_j^2, \quad \sigma_j^2 := \text{Var}_{\eta_j}[Y_{ij}] = 4\eta_j^2\psi^2 + c.$$

To understand the motivation behind this setup, we can further inspect the covariance between  $X_{ij}$  and  $Y_{ij}$ , which can be verified to be  $\text{Cov}_{\eta_j}[X_{ij}, Y_{ij}] = 2\eta_j\psi^2$ . Therefore, if we consider the ratio between the absolute covariance and the variance (of  $Y_{ij}$ ) as a characterization of the “inherent predictability” of a problem, we see that

$$\frac{|\text{Cov}_{\eta_j}[X_{ij}, Y_{ij}]|}{\text{Var}_{\eta_j}[Y_{ij}]} = \frac{2|\eta_j|\psi^2}{4\eta_j^2\psi^2 + c}$$

which has its minimum when  $\eta_j = 0$  and increases monotonically in  $|\eta_j|$  for  $|\eta_j| \in [0, 1]$  given our specific choices of  $\psi$  and  $c$  (see Figure 5). In other words, problems with  $\eta_j$  close to the origin have a lower

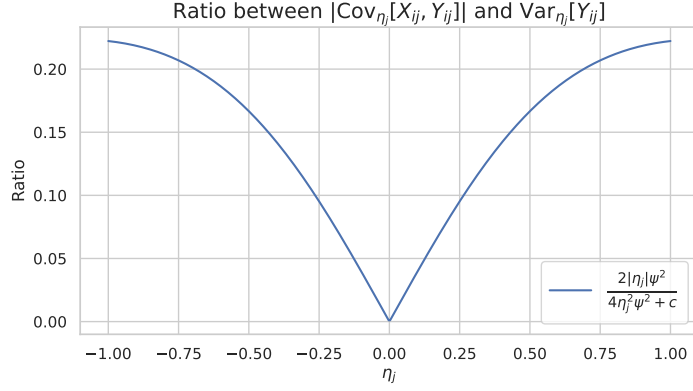


Figure 5: The ratio between  $|\text{Cov}_{\eta_j}[X_{ij}, Y_{ij}]|$  and  $\text{Var}_{\eta_j}[Y_{ij}]$  as a function of  $\eta_j$ . The constants are set to  $\psi = 0.1$  and  $c = 0.05$ .

“predictability;” whereas when  $\eta_j$  moves away from zero, the problems become easier to solve. This quantitatively reflects the pattern we see in Figure 3, where we display the power-tuning parameters as a function of  $\eta_j$ .

**Expressions for  $\theta_j, \mu_j, \sigma_j^2, \tau_j^2, \gamma_j$  when  $f(x) = |x|$ .** When we work with the synthetic model using the flawed predictor  $f(x) = |x|$ , we can match the form of our dataset with the general setting in Assumption 2.2 by identifying closed-form expressions for the model parameters  $\theta_j, \mu_j, \sigma_j^2, \tau_j^2, \gamma_j$ .

$$\begin{aligned}\theta_j &= \eta_j^2, & \sigma_j^2 &= 4\eta_j^2\psi^2 + c, \\ \gamma_j &= 2\eta_j\psi^2\sqrt{\frac{2}{\pi}}e^{-\eta_j^2/(2\psi^2)}, & \mu_j &= \sqrt{\frac{2}{\pi}}\psi\exp\left(-\frac{\eta_j}{2\psi^2}\right) + \eta_j\left[\Phi\left(\frac{\eta_j}{\psi}\right) - \frac{1}{2}\right], \\ \tau_j^2 &= \eta_j^2 + \psi^2 - \left[\sqrt{\frac{2\psi^2}{\pi}}\exp\left(-\frac{\eta_j^2}{2\psi^2}\right) + \eta_j\left(2\Phi\left(\frac{\eta_j}{\psi}\right) - 1\right)\right]^2,\end{aligned}$$

where  $\Phi(\cdot)$  denotes the standard normal distribution function.

**Expressions for  $\theta_j, \mu_j, \sigma_j^2, \tau_j^2, \gamma_j$  when  $f(x) = x^2$ .** Similar closed-form expressions can be derived when we use the other predictor  $f(x) = x^2$ . Note that  $\theta_j$  and  $\sigma_j^2$  remain the same.

$$\begin{aligned}\theta_j &= \eta_j^2, & \sigma_j^2 &= 4\eta_j^2\psi^2 + c, \\ \gamma_j &= 4\eta_j^2\psi^2, & \mu_j &= \eta_j^2 + \psi^2, & \tau_j^2 &= 2\psi^4 + 4\eta_j^2\psi^2.\end{aligned}$$

In experiments involving the synthetic model with both predictors, we are able to leverage these closed-form expressions and supplement the ground-truth parameters to our datasets.

**Interpretation of MSE.** In the synthetic experiments, since we have access to the true prior for  $\eta_j$  (therefore for  $\theta_j$ ) and resample them for each problem across  $K$  trials, the MSE we obtained in Table 2 is an unbiased estimate of the *Bayes Risk* defined in Eq. (11).

### D.3 Amazon Review Ratings Dataset

**Dataset & Preprocessing.** The *Amazon Fine Food Reviews* dataset, provided by the Stanford Network Analysis Project (SNAP; SNAP [2014]) on Kaggle,<sup>11</sup> comes in a clean format. We group reviews by their ProductID. For each review, we concatenate the title and body text to form the covariate, while the response is the reviewer’s score/rating (1 to 5 stars). Here’s a sample review:

<sup>11</sup><https://www.kaggle.com/datasets/snap/amazon-fine-food-reviews>

**Score:** 4

**Product:** BBQ Pop Chips

**Title:** Delicious!

**Text:** BBQ Pop Chips are a delicious tasting healthier chip than many on the market. They are light and full of flavor. The 3 oz bags are a great size to have. I would recommend them to anyone.

We focus on the top  $m = 200$  products with the most reviews for the compound mean estimation of average ratings. This approach mitigates extreme heteroscedasticity across estimators for different problems, which could unduly favor shrinkage-based methods when considering unweighted compound risk. There are a total of 74,913 reviews for all 200 products.

**Fine-tuning BERT.** The Bidirectional Encoder Representations from Transformers (BERT) model is a widely adopted language model for many NLP tasks including text classification [Devlin, 2018]. However, pretraining BERT from scratch is time-consuming and requires large amounts of data. We therefore use the `bert-base-multilingual-uncased-sentiment` model<sup>12</sup> from NLP Town [2023] as the base model, denoted as `BERT-base`. `BERT-base` is pre-trained on general product reviews (not exclusive to Amazon) in six languages. It achieves 67.5% prediction accuracy on a validation set of 100 products ( $\sim 46k$  reviews).

Then, we further fine-tune it on the held-out review data, that is, reviews outside the top 200 products, for 2 full epochs. The fine-tuning is done using Hugging Face’s `transformers` library [Wolf, 2019]. After fine-tuning, the `BERT-tuned` model achieves 78.8% accuracy on the same validation set.

## D.4 Spiral Galaxy Fractions (Galaxy Zoo 2)

**Dataset & Preprocessing.** The Galaxy Zoo 2 (GZ2) project<sup>13</sup> contains a large collection of human-annotated classification results for galaxy images from SDSS. However, instead of having a single dataframe, GZ2 has many different tables—each for subsets of the SDSS raw data. We begin with a particular subset of 239,696 images with metadata drawn from Hart et al. [2016]. Our data cleaning pipeline is inspired by Lin et al. [2021], which removes missing data and relabels the class name of each galaxy image to a more readable format:

**Class Names:** Round Elliptical, In-between Elliptical, Cigar-shaped Elliptical, Edge-on Spiral, Barred Spiral, Unbarred Spiral, Irregular, Merger

In the downstream estimation problems, we consider a galaxy “spiral” if it is classified as one of the three classes ending with “Spiral”, otherwise “non-spiral”. Below we display a few examples of galaxy images. Each image has dimensions of  $424 \times 424 \times 3$ , where the third dimension represents the three filter channels: g (green), r (red), and i (infrared). The cleaned dataset has 155,951 images in total.

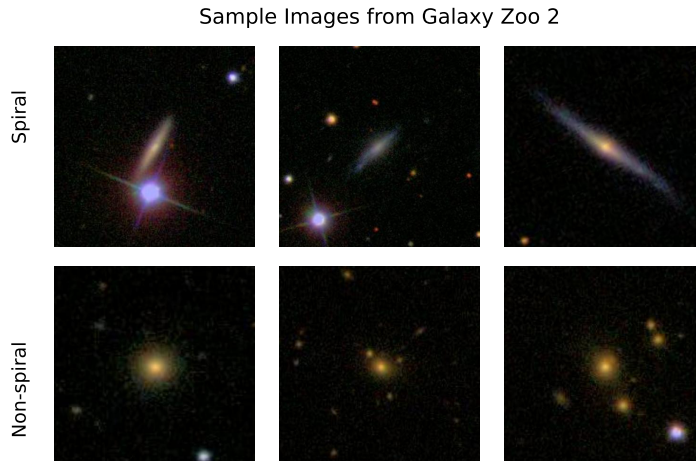


Figure 6: Example of spiral & non-spiral galaxy images from Galaxy Zoo 2.

<sup>12</sup><https://huggingface.co/nlptown/bert-base-multilingual-uncased-sentiment>

<sup>13</sup><https://data.galaxyzoo.org/>

The additional SDSS metadata for GZ2<sup>14</sup> contains valuable information that directly partitions the galaxies based on certain attributes, e.g., REDSHIFT\_SIMPLE\_BIN based on galaxy redshift measurements, and WVT\_BIN calculated by weighted Voronoi tessellation. These partitions naturally motivate fine-grained compound mean estimation on this dataset.

After partitioning the images based on REDSHIFT\_SIMPLE\_BIN,<sup>15</sup> we consider only the top  $m = 122$  partitions based on the cutoff that each problem should have  $\geq 150$  images (many partitions have very few galaxy images in them), for the same reason as in the Amazon Review dataset. Finally, we have a total of  $\sim 100\text{k}$  images as covariates (either  $X_{ij}$  or  $\tilde{X}_{ij}$ ) for our problem.

**Training the Predictor.** We employ the ResNet50 architecture [He et al., 2016], utilizing the pre-trained model from torchvision initially trained on ImageNet [Deng et al., 2009]. To tailor the model to our task, we fine-tune it on  $\sim 50\text{k}$  images excluded from the top  $m$  problems. The model is trained to classify galaxies into eight categories, later condensed into a binary spiral/non-spiral classification for prediction. We use a batch size of 256 and Adam optimizer [Kingma, 2014] with a learning rate of  $1e-3$ . After 20 epochs, the model achieves 87% training accuracy and 83% test accuracy. Despite these promising results, Table 3 indicates that the predictions still require de-biasing for accurate estimation.

## D.5 Benchmarking in real-world datasets

In this appendix we describe the steps to obtain the MSEs and their standard errors for real-world datasets shown in Table 3.

Let  $K$  be the number of experiment trials,  $T_j$  be the total number of data points for problem  $j$ , i.e.  $\{\dot{X}_{ij}, \dot{Y}_{ij}\}_{j=1}^{T_j}$  represents the “raw data” we have, and  $n_j, N_j$  be the desired number of labeled/unlabeled data to simulate, usually calculated through a hyper-parameter splitting ratio (e.g.  $N_j = \lfloor r \cdot T_j \rfloor$ ,  $n_j = T_j - N_j$  for  $r = 0.8$  in our case).

1. Following evaluation methodology in existing PPI literature, e.g., [Angelopoulos et al., 2023], we first calculate the mean of all responses for each problem and treat it as the pseudo ground-truth, i.e.,  $\hat{\theta}_j := \frac{1}{T_j} \sum_i \dot{Y}_{ij}$ .
2. For each trial  $k \in [K]$ , we create a random permutation for the raw data, with indices permuted by  $\kappa : \mathbb{N} \rightarrow \mathbb{N}$ , and obtain the labeled and unlabeled datasets for problem  $j$  as

$$\{X_{ij}, Y_{ij}\}_{i=1}^{n_j} = \{\dot{X}_{\kappa(i)j}, \dot{Y}_{\kappa(i)j}\}_{i=1}^{n_j}, \quad \{\tilde{X}_{ij}\}_{i=1}^{N_j} = \{\dot{X}_{\kappa(i)j}\}_{i=n_j+1}^{T_j}$$

3. We proceed with using these datasets to obtain the baseline and PAS estimators. Let  $\hat{\theta}_j^k$  be an estimator for the  $j$ -th problem at trial  $k$ , then our final reported MSE and standard error is calculated as

$$\widehat{\text{MSE}}_K(\hat{\theta}) := \frac{1}{K} \sum_{k=1}^K \left( \frac{1}{m} \sum_{j=1}^m (\hat{\theta}_j^k - \hat{\theta}_j)^2 \right),$$

$$\text{SE}_K(\hat{\theta}) := \frac{1}{\sqrt{K}} \sqrt{\frac{1}{K-1} \sum_{k=1}^K \left( \frac{1}{m} \sum_{j=1}^m (\hat{\theta}_j^k - \hat{\theta}_j)^2 - \widehat{\text{MSE}}_K(\hat{\theta}) \right)}.$$

It should be noted that the standard error only accounts for uncertainty due to the random splits into labeled and unlabeled datasets.

<sup>14</sup>The column names and their meanings are available at <https://data.galaxyzoo.org/data/gz2/gz2sample.txt>.

<sup>15</sup>In astronomy, REDSHIFT quantifies how much the wavelength of light from a galaxy is stretched due to the expansion of the universe. It serves as a good proxy for grouping galaxies of similar distance and time.

## D.6 Computational Resources

All the experiments were conducted on a compute cluster with Intel Xeon Silver 4514Y (16 cores) CPU, Nvidia A100 (80GB) GPU, and 64GB of memory. Fine-tuning the **BERT-tuned** model took 2 hours, and training the **ResNet50** model took 1 hour. All the inferences (predictions) can be done within 10 minutes. The nature of our research problem requires running the prediction only once per dataset, making it fast to benchmark all estimators for  $K = 200$  trials using existing predictions.

## D.7 Code Availability

The code for reproducing the experiments is available at

<https://github.com/listar2000/prediction-powered-adaptive-shrinkage>.